

DISSERTAÇÃO DE MESTRADO Nº 884

**A MULTIMODAL INVERSE PROBLEM FOR GPR PAVEMENT PARAMETER
ESTIMATION**

Maria Victoria Africano Contreras

DATA DA DEFESA: 04/09/2015

Universidade Federal de Minas Gerais

Escola de Engenharia

Programa de Pós-Graduação em Engenharia Elétrica

**A MULTIMODAL INVERSE PROBLEM FOR GPR PAVEMENT
PARAMETER ESTIMATION**

Maria Victoria Africano Contreras

Dissertação de Mestrado submetida à Banca Examinadora designada pelo Colegiado do Programa de Pós-Graduação em Engenharia Elétrica da Escola de Engenharia da Universidade Federal de Minas Gerais, como requisito para obtenção do Título de Mestre em Engenharia Elétrica.

Orientador: Prof. Ricardo Luiz da Silva Adriano

Belo Horizonte - MG

Setembro de 2015

C764

Contreras, Maria Victoria Africano.

A multimodal inverse problem for GPR pavement parameter estimation
[manuscrito] / Maria Victoria Africano Contreras. – 2015.
xvii, 51 f., enc.: il.

Orientador: Ricardo Luiz da Silva Adriano.

Dissertação (mestrado) Universidade Federal de Minas Gerais,
Escola de Engenharia.

Bibliografia: f. 46-51.

1. Engenharia elétrica - Teses. 2. Radar - Teses. 3. Otimização
combinatória - Teses. 4. Teste de penetração do solo - Teses. I. Adriano,
Ricardo Luiz da Silva. II. Universidade Federal de Minas Gerais. Escola de
Engenharia. III. Título.

CDU: 621.3(043)


**"A Multimodal Inverse Problem for GPR Pavement
Parameter Estimation"**

Maria Victoria Africano Contreras

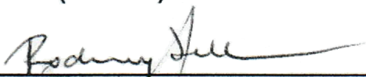
Dissertação de Mestrado submetida à Banca Examinadora designada pelo Colegiado do Programa de Pós-Graduação em Engenharia Elétrica da Escola de Engenharia da Universidade Federal de Minas Gerais, como requisito para obtenção do grau de Mestre em Engenharia Elétrica.

Aprovada em 04 de setembro de 2015.

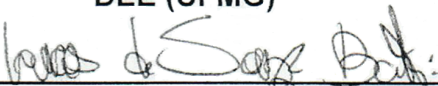
Por:



Prof. Dr. Ricardo Luiz da Silva Adriano
DEE (UFMG) - Orientador



Prof. Dr. Rodney Rezende Saldanha
DEE (UFMG)



Prof. Dr. Lucas de Souza Batista
DEE (UFMG)



Prof. Dr. Douglas Alexandre Gomes Vieira
(ENACOM - Engenharia Assistida por Computador)

To God. Because He has always given me the strength, health and encouragement to achieve all my goals. He will always be my guide.

To my beloved family. Especially to my parents. They have always supported me on each step of my life. Despite the distance, they offer me all the necessary love, company and comprehension to carry out my master study. I owe this professional victory to them.

Also, to my little nieces because they always share their love, smiles and sweetness from the distance.

Maria Victoria Africano Contreras

Acknowledgments

I would like to express my sincere gratitude to my advisor Prof. Ricardo Adriano by the friendly reception, the continuous orientation on my master study, the shared knowledge, and for his patience and motivation.

I take this opportunity to express my gratefulness to all my friends, Colombians and Brazilians, because they are like my family here. They gave me funny and relaxing moments, while encouraged me to strive towards my goal.

In particular, I am grateful to my dear friend Diego Tami because he shared with me the idea to come to Brazil to continue my studies. I know that without him this would not have been possible.

I am also immensely grateful with Brayan Acevedo because his presence was essential to end my master. Thanks for your insights discussing some important concepts. Your company has been valuable and significant to finish this goal with success.

Finally, I would like to thank to CNPq for the financial support given with the scholarship.

“Never forget that you can always surprise yourself.”

Maria V. Africano

Resumo

Nesta dissertação é proposta uma abordagem diferente para determinar a permissividade e espessura de rodovias modeladas como camadas superpostas usando o perfil do subsolo geradas pelo GPR. Deste modo, foi desenvolvido e analisado um algoritmo de otimização, com base em computação evolutiva, que pode ser aplicado para resolver o problema inverso. Por meio da metodologia proposta, pretende-se estimar as propriedades de rodovias proporcionando algumas vantagens que não foram aludidas em estudos anteriores na área.

A estimativa de parâmetros de pavimento usando o radar de penetração do solo é abordado a partir de três diferentes metodologias. Estas metodologias foram simuladas a partir de uma estrutura de pavimento flexível para realizar uma análise comparativa que permitiu destacar as vantagens e desvantagens da sua utilização.

Em primeiro lugar, uma abordagem no domínio do tempo foi feita e os resultados mostraram que o método proporciona uma forma fechada para avaliar os parâmetros de pavimento usando as equações simples. No entanto, demonstrou-se que a precisão deste método é altamente dependente da avaliação dos instantes de reflexão e as amplitudes de pico. A presença de múltiplas reflexões piora o desempenho do método, uma vez que é difícil associar o pulso refletido à sua respectiva interface de onde se origina a reflexão. Além disso, as camadas muito finas geram impulsos sobrepostos que não são detectados facilmente.

Em segundo lugar, uma abordagem de domínio de frequência foi executada minimizando uma função de erro. Neste caso, as características das camadas superpostas não podem ser obtidas em uma forma fechada. O problema da caracterização do pavimento é geralmente tratado como um problema electromagnético inverso, que é normalmente resolvido utilizando algum método de otimização. Os resultados para este método garantiram que o problema estivesse bem posto por meio da definição de uma frequência máxima o qual também resulta em um problema de otimização unimodal na vizinhança do ponto ótimo. Esta característica unimodal proporciona a vantagem de utilizar ferramentas de otimização determinísticas, resultando em métodos de con-

vergência rápida. No entanto, a principal desvantagem relacionada à existência de uma frequência máxima é o tamanho da antena. A definição de uma frequência máxima limita o tamanho mínimo da antena.

Em terceiro lugar, uma variação do segundo método foi sugerida pela autora desta dissertação para tirar vantagens de ambos os métodos já definidos. O problema inverso também foi baseado na minimização da função de erro, de forma semelhante ao descrito na abordagem anterior. No entanto, o sinal utilizado foi um sinal com múltiplas componentes em frequência. Os resultados mostraram que a utilização deste método garante que o problema continue bem-posto sem a restrição de frequência máxima. Os parâmetros do pavimento foram obtidos corretamente. No entanto, uma forte característica multimodal é apresentada na função objetivo que cancela qualquer possibilidade de utilização de ferramentas de otimização determinísticas. Este leva a utilização de algoritmos estocásticos que adiciona complexidade computacional.

Palavras-chave: Radar de Penetração no solo, multicamada, materiais de rodovia, otimização.

Abstract

This thesis proposes a different approach to determine the permittivity and thickness of highways modeled as overlapping layers using the subsoil profile generated by the GPR. In this way, it was developed and analyzed an optimization algorithm based on evolutionary computation that could be applied to solve the inverse problem. By means of the proposed methodology, we intend to estimate the highway properties providing some advantages that wasn't alluded in previous studies in the area.

The pavement parameter estimation using ground penetrating radar is approached from three different methodologies. These methodologies were tested on a flexible pavement structure attempting to perform a comparative analysis that allowed to highlight the advantages and disadvantages of their use.

First, a time domain approach was treated and results showed that the method provides a closed form to evaluate the pavement parameters using single equations. However, it was demonstrated that the accuracy of this method is highly dependent on the evaluation of the reflection instants and the peak amplitudes. The presence of multiple reflections worsens the method performance, since it is difficult to associate the reflected pulse to its respective interface where the reflection originates. Moreover, very thin layers generate overlapped pulses that are not easily detected.

Secondly, a frequency domain approach was performed minimizing an error function. In this case, the characteristics of the multiple layers could not be obtained in a closed form. The problem of pavement characterization is usually treated as an electromagnetic inverse problem, which is usually solved using some optimization method. Results for this method guaranteed that the problem was well-posed by means of the definition of a maximum frequency which also results in a unimodal optimization problem in the optimum point vicinity. This unimodal characteristic gives the advantage of using deterministic optimization tools, resulting in fast convergence methods. However, the main drawback concerning the existence of a maximal frequency is the size of the antenna. Setting a maximal frequency limits the minimal size of the antenna.

Finally, a third approach was suggested by the author of this thesis to take ad-

vantages of both methods already defined. The inverse problem was also based on minimizing the error function, similarly to what was described on the previous approach. Nevertheless, the used signal was expanded to include multiple frequency components. Results showed that using this method it is guaranteed: the well-posedness of the problem without the maximal frequency restriction and that the pavement parameters were properly obtained. However, a strong multimodal characteristic is presented in the objective function which cancel any possibility of using deterministic optimization tools. This leads to the use stochastic algorithms that adds computational complexity.

Palavras-chave: Ground Penetrating Radar, multilayer, high-road materials, optimization.

List of Figures

2.1	General definition of forward and inverse problems	8
2.2	Reflected and transmitted waves with normal incidence	11
2.3	Reflection and transmission in multiple layers with normal incidence	11
2.4	Pavement Structure Types	14
2.5	General composition of typical roads.	15
3.1	Local and Global minimums over unimodal and multimodal functions	19
3.2	Flowchart of the differential evolution algorithm	22
4.1	GPR trace simulated using FDTD method at 9 GHz	26
4.2	GPR trace simulated using FDTD method at 1 GHz	30
4.3	Electric reflected field pulses at two different frequencies	30
4.4	GPR measurement adding random noise	31
4.5	Error function and layer thickness relation	33
4.6	Error function and relative permittivity relation for 200 MHz and 1.5 GHz	34
4.7	Error function vs. ϵ_1 and d_1 for the maximum frequency value (600 MHz)	35
4.8	Error function vs. ϵ_1 and d_1 for a frequency value lower than maximum (200 MHz)	35
4.9	Error function and layer thickness relation for two different GPR frequencies	36
4.10	Error function vs. ϵ_1 and d_1 for a frequency summation (500 MHz - 2.5 GHz)	38
4.11	Level curves and best estimated value of two variables for a frequency summation with $f_c = 1.5GHz$	39
4.12	Better error function by generation for two variables using a frequency summation with $f_c = 1.5GHz$	40
4.13	Better error function by generation for 5 variables using a frequency summation with $f_c = 1.5GHz$	41
4.14	Better error function by generation for 5 variables using a frequency summation and a signal random noise.	42

List of Tables

2.1	Typical materials values used in road construction	16
3.1	Pavement materials pavement selected as reference	24
4.1	Results using time domain approach	28
4.2	Percentage error values for GPR reflected electric field signal simulated with white random noise at 9 GHz	31
4.3	Thickness limits, reference permittivity and computed maximum frequency	36
4.4	Reference model and algorithm results	40
4.5	Percentage quadratic error for third approach	41
4.6	Results of the complete problem with random noise	42

List of Symbols

\mathbf{E}_i	Incident electric field (V/m)
\mathbf{E}_0	Incident electric field Amplitude (V/m)
\mathbf{E}_r	Reflected electric field (V/m)
\mathbf{E}_t	Transmitted electric field (V/m)
\mathbf{E}_{GPR}	Reflected electric field measured with the GPR (V/m)
\mathbf{H}_i	Incident magnetic field (A/m)
\mathbf{H}_r	Reflected magnetic field (A/m)
\mathbf{H}_t	Transmitted magnetic field (A/m)
Γ_0	Reflection coefficient at the boundary
T_0	Transmission coefficient at the boundary
β_1	Phase constant of medium 1
β_2	Phase constant of medium 2
η_1	Intrinsic impedance of medium 1
η_2	Intrinsic impedance of medium 2
μ_0	Magnetic permeability in the air (H/m)
μ_{r1}	Relative magnetic permeability of medium 1 (H/m)
μ_{r2}	Relative magnetic permeability of medium 2 (H/m)
ϵ_0	Electric permittivity in the air (F/m)
ϵ_{r1}	Relative dielectric permittivity of medium 1 (F/m)
ϵ_{r2}	Relative dielectric permittivity of medium 2 (F/m)
A_m	Amplitude of the inverse incident GPR signal
t_0	Time shift
τ	Width of the Gaussian pulse
c	Velocity of light

List of Abbreviations

DT	Destructive Techniques
DCP	Dynamic Cone Penetrometer
NDT	Non-Destructive Techniques
GPR	Ground Penetrating Radar
EM	Electromagnetic
CMP	Common Middle Point
TOD	Time of Delay
ANN	Artificial Neural Network
ANTT	Agência Nacional de Transportes Terrestres
DE	Differential Evolution Algorithm
HMA	Hot-Mix Asphalt
PCC	Portland Cement Concrete
ACO	Ant Colony Optimization
AIA	Artificial Immune Algorithm
GA	Genetic Algorithm
PSO	Particle Swarm Optimization
EA	Evolutionary Algorithms
DDE	Dynamic Differential Evolution
FDTD	Finite-Difference Time-Domain

Contents

Acknowledgments	vi
Resumo	viii
Abstract	x
List of Figures	xii
List of Tables	xiii
List of Symbols	xiv
List of Abbreviations	xv
1 Introduction	1
1.1 Motivation	1
1.2 Current GPR State of Knowledge	3
1.3 Potential advantages of using GPR for pavement evaluation	6
1.4 Objectives and Contributions	6
1.5 Survey of chapters	7
2 Problem Contextualization	8
2.1 Mathematical Model	8
2.1.1 Direct/Forward Problem	9
2.1.2 Inverse Problem	12
2.2 Model parameters	14
2.2.1 Pavement structure selected	15
3 Optimization	17
3.1 General optimization definitions	18

3.2	Differential Evolution Algorithm (DE)	19
3.2.1	Method Description	21
3.3	Inverse Pavement problem	23
3.3.1	The reference problem	23
4	Approach Methods and Results	25
4.1	Time Domain approach	25
4.2	Frequency Domain approach	31
4.3	Multiple frequency approach	37
4.3.1	Optimization of the first layer	38
4.3.2	Complete problem	39
4.3.3	Complete problem with white random noise	41
5	Conclusions	43
5.1	Further Work	44
	Bibliography	46

Chapter 1

Introduction

1.1 Motivation

Traditionally, Destructive Techniques (DT) have been used to estimate the pavement layer thickness using several procedures as digging test-pits, extracting cores from pavement and using measurements of the Dynamic Cone Penetrometer (DCP) [Khoury et al., 2014, Brough et al., 2003, Hartman et al., 2004, Zumrawi, 2014]. As its name suggests, DT uses samples of the ground for, later, perform a respective analysis in a laboratory. This offers the advantage of a visual inspection which is essential to evaluate pavement structures from a geotechnical point of view. However, all of these procedures have shown some disadvantages in its implementation and execution. Generally, they consume a lot of time and money and can cause big traffic jams, especially on highways, because the examined lane needs to be closed. Also, the implementation of DT contributes to a rapid deterioration of the pavement structure. For instance, extracting cores for roads might cause weakening of the entire area surrounding the core locations. As a consequence, Non-Destructive Techniques (NDT) have become important for quality control of many structures, since it only requires measurements made from road surface and, as a result, they do not compromise the pavement condition.

A well-accepted NDT is the Ground Penetrating Radar (GPR), a geophysical technique widely used on researches about subsoil which is a good approach to solve the possible problems presented in many fields, such as: archeology, geophysics, engineering, among others [Iswandy et al., 2009, Gomez López, 2008]. The technique is commonly used for construction and maintenance of highways where the estimation of the layers characteristics is important for evaluating the quality of roads or railways. In broad terms, the GPR uses a transmitter antenna (T_x) to send a short electromagnetic pulse with a specific frequency, varying from 50 MHz up to 2.5 GHz, to the

surface [Morey, 1998]. If there is an object or variation on the electrical properties of the materials that compose a road (discontinuity), it will cause wave reflections. Then, these will be detected by a receiver antenna (R_x). Thus, a continuous profile of the subsurface is obtained while the radar is moving on and the data will be saved to a posterior analysis.

All Ground Penetrating Radar can be classified depending on the type of antenna used. In this way, they can be categorized as air-coupled or ground-coupled. The difference between these two systems is the existing distance from the antenna position to the surface to be analyzed. For the air-coupled mode, the antennas are situated about 250 mm above the surface, allowing operation at highways speed (up to 80 km/h approximately). In a different way, ground-coupled antennas are at a small distance from surface (just a few millimeters). In this case, the speed will be limited to 8 km/h approximately [Loizos and Plati, 2007]. The antenna size is closely related with the radar operation frequency; the smaller the antenna, the higher the frequency. Consequently, the GPR resolution increases and the depth reached decreases [Morey, 1998]. Many applications have characteristics that can be modeled as multiple layers arrangements.

In the highways and railroads case, the subsoil can be represented as a set of overlapping layers with specific constitutive parameters which will change according to the material they are made of [AL-Qadi and Lahouar, 2005]. Therefore, variations in the structure of roads can be identified by means of variations in the layers' dielectric properties [Morey, 1998].

Obtaining the layers' characteristics from the signals acquired with the GPR represents an inverse electromagnetic problem which can be solved using two wide approaches: frequency and time domain techniques [Queiroz et al., 2013].

- (a) The frequency domain techniques [Hunaidi, 1998, Oliveira et al., 2014] make use of optimization tools to solve the problem, but this implies a great difficulty in ensuring uniqueness in the solution.
- (b) The time domain techniques [Loizos and Plati, 2007, Lahouar and Al-Qadi, 2008] generally use the wave travel time between the layers to define their dielectric properties. However, the quality of results depends on the right detection of the reflection peaks measured by GPR that can't be easily described if the signal is affected by some noise or interference. All this analysis will be discussed deeply later.

To sum up, it is necessary the development of methodologies capable of solving the inverse problem generated by the wave propagation over multiple layers to elaborate non-destructive tests using electromagnetic radiation. This thesis intends to analyze the advantages and disadvantages of traditional approaches and, additionally, it proposes a methodology based on the spectral analysis of the reflected signal in order to solve the electromagnetic inverse problem.

1.2 Current GPR State of Knowledge

GPR Applications to Pavements

According to the literature, a GPR system could be used for roads structure evaluation as a quality control tool. In this manner, GPR can be used to check newly constructed pavements and evaluate the existing ones [Saarenketo and Scullion, 2000]. These two main GPR functions have been addressed in many studies.

The study presented in [Benedetto and Benedetto, 2002] uses different GPR responses in respect to the water content in order to find how the soil moisture and density affect the dielectric value at different frequency. The materials' dielectric value were measured in the laboratory considering lower water sensitive materials, sandy and pozzolanic road sub-grades. It was concluded that there is a relevant correlation between moisture and relative dielectric constant and a significant correlation between dielectric properties and soil density. Also, it was noted that the sensibility is greater for higher frequencies in the diagnosis of sub-grade compaction status. The survey couldn't provide any reliable generalization yet, but results were promising to have a diagnostic tool able to identify the main causes of road pavement damage.

GPR investigations were used in [Colagrande et al., 2011] to study degraded road flexible pavements built in cutting sections. The analysis was done by comparing damaged and undamaged road pavement sites, they were assessed via quantitative analysis of power curves through the rectified power method and the subsequent determination of the absorption coefficient α . It was concluded that when the absorption angles of damaged and undamaged road sections are similar, then the likely cause of degradation is fatigue or thermal shrinkage; when they are not, then the triggering factor of road degradation is the different compactness of the soil caused by vehicular traffic load. Also, results pointed out that the accuracy of interpretation of the 1600 MHz sections depends on the resolution provided by the antenna working frequency and on the sampling rate of the radar signal.

The matched filter technique and the derivative technique for finding road layer

thicknesses and dielectric constants using data collected by GPR were studied in [Kurtz et al., 2006]. The used pavement model incorporates multiple layers and the data analysis iteratively detects all the reflected pulses from time domain signal. Then, dielectric constants are computed using the reflection amplitudes, without taking into account material loss, and the layer thicknesses are estimated based on the travel times and the corresponding electromagnetic speed in each layer. After an evaluation with added noise, results showed that the matched filter technique generally worked better than the derivative technique. However, it won't reliably detect very thin layers (<25.4 mm) or multiple, adjacent thin layers (~ 25.4 mm).

Two inverse scattering approaches were addressed by Spagnolini [Spagnolini, 1997] to estimate permittivity profiles, pavement thicknesses and concrete deterioration for programmed road and bridge deck maintenance, using multiple layers in the pavement model. The first approach was a layer-stripping algorithm that used the amplitude and time delay of radar echoes after their detection. The second was an EM inverse problem or parameter optimization in the time domain by minimizing the mean square error between measured and modeled data, implementing the Gauss-Newton method. It was assumed laterally smoother permittivity variations than antenna beamwidth, so the content of any diffraction or laterally reflected energy were negligible. The reliability of the methods proposed was validated with core samples, achieving less than 8 % error in thickness estimation. Results proved that layer stripping inversion represents a useful and efficient technique for interface profiling. Nevertheless, it presents some drawbacks as misses or false alarms in interface tracking, errors in amplitude estimation, and significant errors in permittivity model. Now, in the inversion procedure, it was obtained a good result when it was used adequate material loss values. However, it is computationally intensive.

In [Gentili and Spagnolini, 2000], it was also used the same inversion technique of [Spagnolini, 1997] but the reflected signal was obtained by using a frequency domain model, instead of the time domain model. This one was preferred for computational convenience since it is directly related to the forward modeling approach. Results of this system was comparable to Spagnolini's one.

Fauchard *et al.* [Fauchard et al., 2003] performed GPR profile experiments for 7 different road structures with the purpose of estimating the permittivity and thickness of an asphalt multi-layered pavement. The studied approaches included the use of cores, the laboratory permittivity measurements and the Common Middle Point (CMP) method [Bohidar and Hermance, 2002]. Using the cores approach, the readability of thicknesses on a core was limited by the size of the largest aggregates, thus the accuracy is also limited. Besides, it was mentioned various parameters to be taken into account

when GPR measurements are concerned. The permittivity measurements, obtained from cores, were taken on the same GPR frequencies in order to be able to establish comparisons between two destructive approaches. Finally, the CMP method intended to estimate the pavement parameters attempting to avoid cores. It uses the Time of Delay (TOD) corresponding to each layer. Results of these three approaches presented accuracies within those specified for road construction and maintenance needs, as well as for the acceptance of road work.

Molyneaux [Molyneaux et al., 1995] attempts to detect the presence, size and the depth of a rebar by means of the interpretation of reinforced concrete radar images using Artificial Neural Networks (ANN). The network used is composed of three fully connected layers. The Fourier transform of the received signal over the center of the rebar is used by the ANN as input nodes. The output was formed by seven nodes where the first output node represented the rebar presence (1) or absence (0). Whereas, the other six represented 6 possible rebar depths (25 mm, 50 mm, 100 mm, 155 mm, 200 mm or 260 mm). Then, a number 1 is shown in the estimated depth. All of the radar results handled for this study were taken from a water-oil emulsion tank (which was shown to have same electromagnetic properties as structural concrete) and steel rebar at different depths. The tests displayed a failure rate of 42% when it wrongly detected the rebar presence.

Other studies covering the ANN usage for the estimation of GPR surveys are [Rodriguez et al., 2015] [Queiroz et al., 2012]. In [Rodriguez et al., 2015], they use techniques based on Principal-Component Analysis (PCA) and NNs to build prediction systems in GPR-based geological surveys. The applied algorithm outperforms previous NN predictors, achieving a high-rate of success. Now, efficient inverse methods to GPR raw concrete data were exposed in [Queiroz et al., 2012]. The survey describes alternative ways of solving the inverse problem of retrieving buried inclusions in dielectrics with similar electrical characteristics to concrete slabs. ANNs were employed to solve a 2D problem where a cylinder of unknown characteristics is buried in a non-homogeneous dielectric. The incident and scattered wave were simulated using FDTD to train the ANN. Also, in order to reduce the dimensionality of the problem, Principal Component Analysis (PCA) was used along with ANN. In this way, it allows the data to be compressed, which means that the dimensions number is reduced without much information loss.

1.3 Potential advantages of using GPR for pavement evaluation

We already mentioned how important it is to perform an accurate layer thickness estimation for the different working areas in the construction and supervision of pavements. Mainly, the right measurement of the layer thicknesses will ensure that the pavement complies with the design specifications helping to exercise quality control.

Traditional Destructive Techniques are based on observations of a finite number of cores taken from the lane under evaluation, which leads to three main drawbacks: first, pavement structure could present, with time, weakness around the extracted cores locations. Second, since this evaluation is done over a small set of points, DT are not very representative for the entire pavement. Finally, DT are time-consuming and require the working area to be closed. This characteristic does not represent an economical technique, especially when highways are intervened.

According to the 2013 annual report of the "Agência Nacional de Transportes Terrestres" (ANTT) [Agência Nacional de Transportes Terrestres, 2013], R\$42 billions would be invested in Brazil to perform maintenance, construction and rehabilitation of public roads structures. The maintenance costs reduction would be considerable if the non-destructive evaluation techniques were introduced to improve the efficiency of the decision-making process, taking advantage that they are reliable and easy to use. Such improvement can be offered by the Ground Penetrating Radar. In fact, it is a prospective and non-destructive tool, it can be used at highway speeds and offers useful information about the pavement being evaluated.

1.4 Objectives and Contributions

The present work proposes a different approach to determine the permittivity and thickness of highways modeled as overlapping layers using the subsoil profile generated by the GPR. We used and reproduced the results of two interesting researches [Oliveira et al., 2014, Loizos and Plati, 2007] with the purpose of performing a comparative study of methods in time and frequency domain. The objective of this thesis is the development and analysis of an optimization algorithm, based on evolutionary computation, that could be applied to solve the inverse problem. We believe that this is a significant contribution because we suggest another methodology to define the highways properties providing some advantages that weren't alluded in previous studies in the area. The obtained results in this thesis generated an article that was published in the MOMAG

2014 (16° SBMO - Simpósio Brasileiro de Micro-ondas e Optoeletrônica e 11° CBMag - Congresso Brasileiro de Eletromagnetismo) [Africano and Adriano, 2014].

1.5 Survey of chapters

This thesis is organized in 5 chapters. The second chapter contains the definitions and mathematical concepts of the direct and inverse electromagnetic problems used in the pavement characterization. Also, it presents the different types of existing pavements and the pavement selected, as reference problem, to perform an adequate evaluation of the approaches analyzed in this work.

Chapter 3 describes the foundations and basic concepts of optimization. Besides, it presents some previous researches that used Differential Evolution (DE) algorithm and its general description. At the end of this chapter is specified the inverse pavement problem along with the respective reference problem defined. Then, in chapter 4, the description and results of three different methodologies are presented in order to compare them and establish their strengths and weaknesses. Section 4.1 shows the time domain approach to solve the pavement parameters estimation problem. Section 4.2 contains an approach in the frequency domain method considering the use of a maximum frequency limit, and, finally, section 4.3 presents the proposed method of this work which intends to take benefits of both methods. The main conclusions and continuity proposals are described in the last chapter.

Chapter 2

Problem Contextualization

In this chapter, the general concepts of direct and inverse problems are given, along with the basic equations that characterize the direct electromagnetic problem used to analyze the structure of the layers. Also, the pavement types are described in order to select a pavement structure that allows to evaluate the different approach methods under the same criteria.

2.1 Mathematical Model

In a broad and ideal definition, forward problems use a given model with its own parameters m , in order to estimate data values d . In contrast to that, inverse problems intend to reconstruct the model, attempting to estimate the model parameters, from measured data (See Fig. 2.1).

In other words, inverse problems use the observations or measurements with the purpose of constraining the solution of some problem of interest. The model covers the mathematical laws (or another extra information) to find the numerical quantities (model parameters) that it is wanted to estimate. Although, in an ideal case, an exact theory exists that prescribes how the data should be transformed in order to reproduce

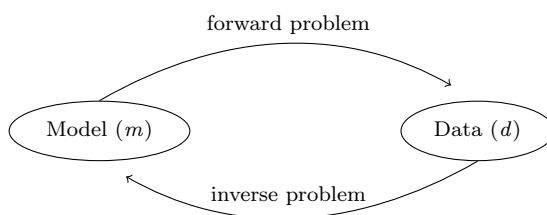


Figure 2.1: General definition of forward and inverse problems

the model in most real applications. There is a bit of freedom in the way model parameters are chosen, generating in this way different solutions for the same problem.

According to this definition, for this study, the direct problem can be defined as the use of electromagnetism laws for estimating the reflected electric field (d) that would be detected by a GPR in the presence of a pre-defined layered pavement. Also, it was mentioned that the inverse problem has the opposite definition of the direct problem. However, it wasn't mentioned that the analysis done in the direct problem can be harnessed to try to solve the inverse one. The detailed analysis to the direct problem is specified in the section 2.1.1 and some important characteristics of inverse problems in section 2.1.2.

2.1.1 Direct/Forward Problem

Electromagnetic scattering appears when the incident wave finds a discontinuity in the material electromagnetic properties of the medium where it is propagating. Such discontinuity will cause the wave present reflection, refraction or diffraction depending on the discontinuity geometry and material properties [Bush, 1989]. Assessment on pavements using GPR consider roads as planar layered media, consequently, it will present only scattering from planar interfaces caused by the interfaces between two layers in a pavement system.

Scattering from planar interface can be represented as shown Fig. 2.2, considering that the wave travel is perpendicular to the planar interface of two semi-infinite mediums (normal incidence). As depicted, the incident wave E_i is partially reflected E_r and partially transmitted E_t according to the change from one medium to another, since they present different electrical properties. The equations of this EM waves can be summarized by Eqs. (2.1) and (2.2). Assuming \hat{x} polarization

$$E_i = E_0 e^{-j\beta_1 z} \hat{x} \quad (2.1a)$$

$$E_r = \Gamma_0 E_0 e^{j\beta_1 z} \hat{x} \quad (2.1b)$$

$$E_t = T_0 E_0 e^{-j\beta_2 z} \hat{x} \quad (2.1c)$$

$$H_i = \frac{E_0}{\eta_1} e^{-j\beta_1 z} \hat{y} \quad (2.2a)$$

$$H_r = \frac{\Gamma_0 E_0}{\eta_1} e^{j\beta_1 z} - \hat{y} \quad (2.2b)$$

$$H_t = \frac{T_0 E_0}{\eta_2} e^{-j\beta_2 z} \hat{y} \quad (2.2c)$$

where E_0 is the amplitude of the incident wave, $\beta_{1,2}$ is the phase constant of medium 1 and 2 respectively and $\eta_{1,2}$ is the intrinsic impedance of medium 1 and 2 respectively. For these two mediums case, $\beta_{1,2}$ and $\eta_{1,2}$ are defined by Eqs. (2.3)

$$\beta_{1,2} = 2\pi f \sqrt{(\mu_0 \mu_{r_{1,2}})(\epsilon_0 \epsilon_{r_{1,2}})} \quad (2.3a)$$

$$\eta_{1,2} = \sqrt{(\mu_0 \mu_{r_{1,2}})/(\epsilon_0 \epsilon_{r_{1,2}})} \quad (2.3b)$$

The reflected and the transmitted electric fields are related to the incident wave by the Fresnel reflection coefficient (Γ_0) defined in Eq. (2.4) for two mediums. This coefficient is a function of the frequency and dielectric properties.

$$\Gamma_0 = \frac{\eta_2 - \eta_1}{\eta_2 + \eta_1} \quad (2.4a)$$

$$T_0 = 1 - \Gamma_0 \quad (2.4b)$$

Now, for GPR data interpretation purposes, any pavement structure can be modeled as a multi-layered system which is composed by consecutive planar layers as shown in Fig. 2.3. Therefore, from the point of view of the electromagnetic theory, it can be analyzed like a multiple interface scattering problem.

The relative permittivity or dielectric constant (ϵ_r) of a material defines the electric polarization grade of a medium when this is subjected to an external electric field. Subsoil materials don't have much capacity to polarization, they are restricted to certain directions of vibration in terms of the electric field vector. However, the existence of water in a determined medium increases the capacity of polarization on it. Since we

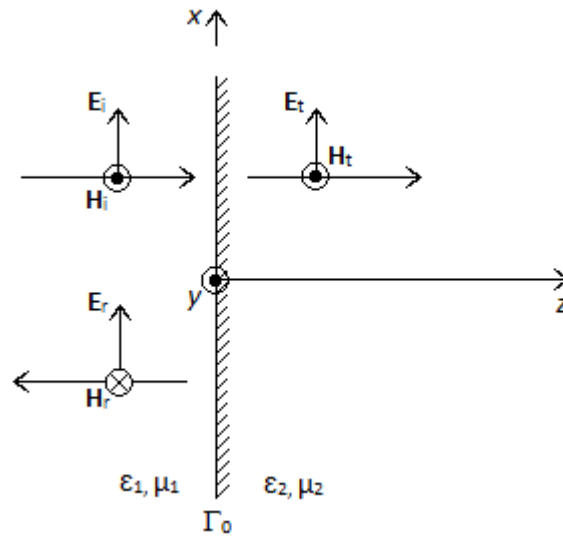


Figure 2.2: Reflected and transmitted waves with normal incidence

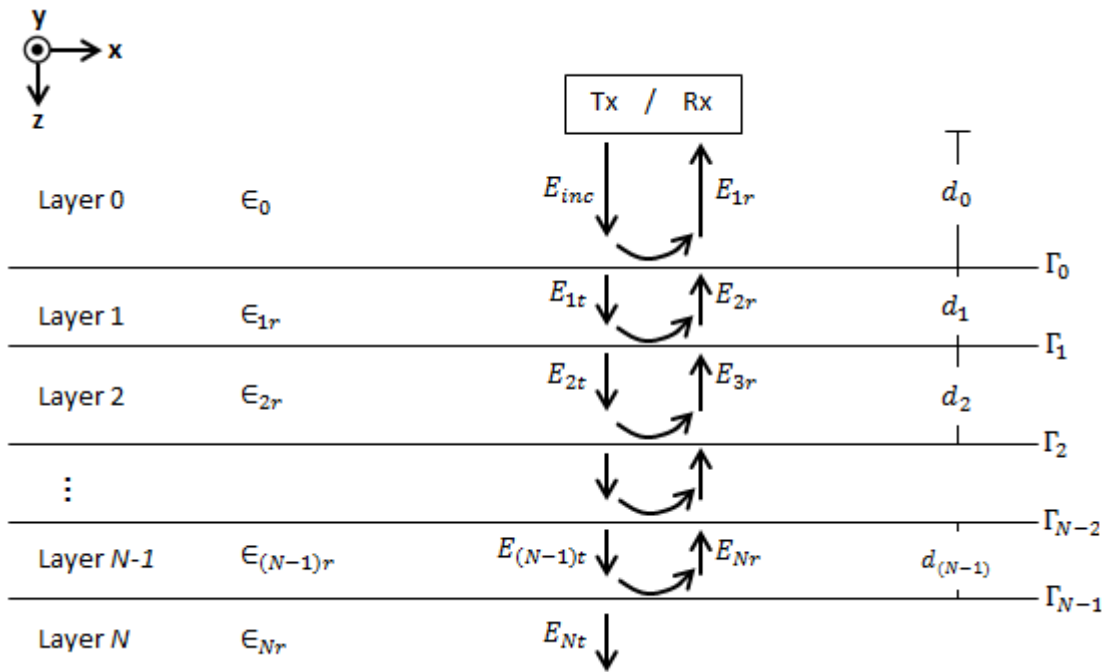


Figure 2.3: Reflection and transmission in multiple layers with normal incidence

are considering dry roads, the permittivity and conductivity on pavement layers is low which allows to have better conditions for wave propagation in the mediums. Then, losses originated by conductivity and polarization are not considered in this study.

The forward/direct problem intends to deduce the reflected electric field as a function of the interest parameters of this survey, thickness (d) and permittivity (ϵ).

Consequently, assuming a plane wave incident field, the problem can be solved analytically using a well-known methodology [Balanis, 1989]. The reflected electric field received by the antenna considering a plane wave normal incidence and n layers is defined by the following equations:

$$E_r = \Gamma_{in} E_i \quad (2.5)$$

where E_i is the incident electric field generated by GPR, E_r is the computed electric field and Γ_{in} is the reflection coefficient for the system of Fig. 2.3 referenced at the first interface. This can be written approximately as

$$\Gamma_{in} = \Gamma_0 + \Gamma_1 e^{-j2\beta_1 d_1} + \Gamma_2 e^{-j2(\beta_1 d_1 + \beta_2 d_2)} + \dots + \Gamma_N e^{-j2(\beta_1 d_1 + \dots + \beta_N d_N)} \quad (2.6)$$

where Γ_0 is the reflection coefficient from interface 1 and N represents the layers number varying from 1 to N . The reflection coefficients at each interface are represented by Γ_N which is defined in this way,

$$\Gamma_N = \frac{\eta_N - \eta_{N-1}}{\eta_N + \eta_{N-1}} \quad (2.7)$$

$N = [1, 2, \dots, N]$. η_L are the impedances of the N -th layers.

$$\eta_L = \sqrt{\mu_0 / \epsilon_0 \epsilon_{Lr}} \quad (2.8)$$

$$\beta_L = 2\pi f \sqrt{\mu_0 (\epsilon_0 \epsilon_{Lr})} \quad (2.9)$$

$L = [1, 2, \dots, L]$. ϵ_{Lr} is the relative permittivity of each layer (L), μ_0 and ϵ_0 are respectively the permeability and permittivity in the air.

2.1.2 Inverse Problem

Inverse methods have been applied in many branches of physical science [Hoffmann et al., 1993, Keilis-Borok and Yanovskaya, 1995, Pastorino, 1998, Pascual-Marqui, 1999, Pastorino et al., 2002, Markel et al., 2003, Benedetti et al., 2006]. The reason is that important properties of media under study can be known by solving this kind

of problem. Particularly, in the pavement condition survey (the area that will be prioritized in this study), it has been used due to the necessity to understand and know the interior of the pavement structure, which is not observable directly, only starting from measured data at the surface.

Menke [Menke, 1989] defined the inverse theory as an organized set of mathematical techniques to obtain useful information about physical world on the basis of inferences drawn from observations. This useful information will be stated in terms of the numerical values of specific properties of the world. The properties are the "model parameters" because it is assumed that there is some specific method (usually a mathematical theory or model) for relating the model parameters to the data. Based on this definition, it is possible to note that the inverse problem contrasts with the forward problem.

Normally, inverse problem presents more difficulty to solve than its corresponding direct problem due to some drawbacks. Inverse problems have its limitations since it is inherently mathematical. Comparing it with the forward problem, we can realize that this has a unique solution and the inverse problem may not have, which implies that a set of different parameters can satisfy the model or measurements. This is because the geophysics problems are indeterminate due to measurement uncertainties and model imperfections [Tarantola, 2005].

The existence of uniqueness in an inverse problem generates a well-posed characteristic. Besides uniqueness, there are two other conditions that can determine if a problem is well-posed or not. For instance, the problem $K(x) = y$ will be well-posed if it has [Travassos et al., 2009]:

1. Existence: $\forall y \in Y, \exists x \in X$ that $K(x) = y$.

In this matter, maybe, there is no model that fits the given data due to an approximate mathematical model or noise contained in the data.

2. Uniqueness: $K(x_1) = K(x_2) \Rightarrow x_1 = x_2$.

If exact solutions to the inverse problem exist, even for an infinite number of exact data, these solutions may not be unique.

3. Stability: given $x_n \subset X$, if $K(x_n) \rightarrow K(x)$ in Y , then $x_n \rightarrow x$ en X .

Often, there is high instability in computing an inverse solution. Namely, that a small change in measurement can lead to big changes in the implied models.

Unfortunately, inverse problems are very susceptible to be ill-posed because they violate at least one of the enumerated properties.

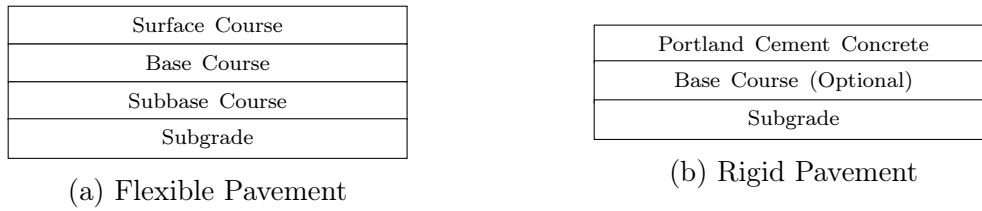


Figure 2.4: Pavement Structure Types

2.2 Model parameters

The pavement structure can be defined as the union of layers placed one upon another, horizontally, used as running surface for the vehicles, rolling stocks or pedestrians. They used different composed materials for each layer. There are two types of pavements to be constructed based on their main components: flexible (hot-mix asphalt) pavements, rigid pavements (concrete) and composite pavements.

- **Flexible pavements:** this pavement type receives its name because it can deflect or flex when there is any traffic loading. Generally, for this type, it is used the best material on the first layer where the intensity of stress, caused by traffic, is high and inferior materials at the bottom due to low intensity. This kind of arrangement usually results in an economical design allowing the use of cheaper local materials in pavement construction [Huang, 2004]. As depicted in Fig. 2.4 (a), the basic structural elements are surface course, base course and subbase course. The surface course is the top layer, constructed by a hot-mix asphalt (HMA) material, which provides a high resistance to big traffic loads. The base course is the layer directly beneath the top one, typically constructed from aggregates such as lime rock, which will not be affected or damaged by humidity. Finally, between the base course and the subgrade, the subbase course is found, which provides structural support using low materials. However, this layer is not always needed or used.
- **Rigid pavements:** this kind of pavement transmit the forces directly to the ground in a minimized form and it is self-resistant. They are constructed using a Portland Cement Concrete (PCC) slab over a base, or directly on the subgrade as shown in Fig. 2.4 (b).
- **Composite or semi-rigid pavements:** this type takes advantage of the two types mentioned above using the most desirable characteristics of the concrete slab, which provides a strong base, and of the flexible layer, which offers smoothness.

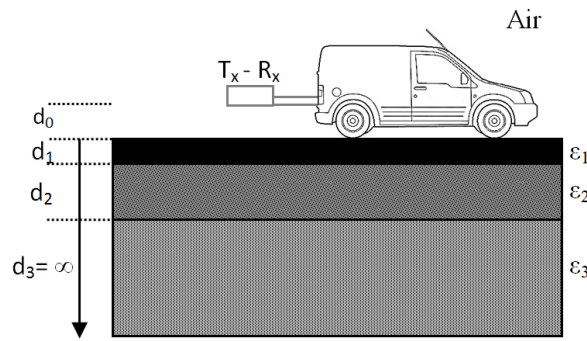


Figure 2.5: General composition of typical roads.

In contrast to this, this kind of pavement is considered high cost and, thus, rarely used for new constructions.

In any case, only a few layers are used to characterize the pavement structure selected.

2.2.1 Pavement structure selected

This section aims to describe the reference environment model that will be used to establish, over same conditions, the behavior of the methods to be studied. We will test them on a typical situation using a usual pavement structure [Lahouar and Al-Qadi, 2008] which is modeled by a set of layers with specific dielectric characteristics and thickness for each one. The highway composition and how it is usually represented is shown in Fig. 2.5.

For this work, we are setting the range of interest for three layers as seen in the Fig. 2.5 (flexible pavement). The layers correspond to surface (layer 1), base (layer 2) and sub-grade (layer 3) courses. In Fig. 2.5, $T_x - R_x$ represents the transmitter and receiver antenna respectively, d_0 is the distance between the first interface and the antennas, $d_{1,2,3}$ and $\epsilon_{1,2,3}$ are the thickness and the permittivity of each layer, respectively.

It should be noted that the permittivity or dielectric constant, ϵ_r , is usually complex. Its real part represents the energy storage in the medium and its imaginary part represents the loss caused by dielectric effects. However, the dielectric constant can be considered as a real number because it depends on the frequency of the EM waves and, it has been proved that, in GPR bandwidth, the permittivity of pavement materials does not vary significantly [Sutinen, 1992]. Therefore, dielectric constant values can be considered as a constant (versus frequency) [Loulizi et al., 2003] to facilitate data interpretation.

The typical values of permittivity (ϵ_r) and thickness (d) that characterize the material used in each road layer are defined in Table 2.1 [Maharaj and Leyland, 2010], [Saarenketo and Scullion, 2000] and [Hidalgo et al., 2010].

Layer	ϵ_r (F/m)	d (cm)
1. Asphalt	2 - 12	6 - 10
2. Base	5 - 10	20 - 30
3. Sub-grade	10 - 25	—

Table 2.1: Typical materials values used in road construction

Chapter 3

Optimization

This chapter shows a general view of optimization tools frequently used in the solution of inverse problems.

Optimization is a process widely studied in many fields like mathematics, statistics, economics and computer science. Optimization methods use algorithms and models from mathematics and statistics in the attempt to find the minimum or maximum value of a function, known as objective function, under certain constraints [Bazaraa et al., 2006].

There are many optimization problems solved using diverse optimization algorithms. They can be classified in two groups: deterministic and stochastic methods [Onwubolu and Babu, 2013]. Traditional methods such as steepest descent, linear programming and dynamic programming are helpful to solve continuous and differentiable functions. They allow us to know properly the minimum or maximum points in a function and if the applications of this technique are still going strong. However, most of the traditional techniques are generally unsuccessful solving large-scale problems, especially with nonlinear objective functions. They require gradient information and hence it is not possible to solve non-differentiable functions. Additionally, such techniques often fail to solve optimization problems that have many local optima [Rao and Savsani, 2012]. To overcome all these problems, it has become important to implement more effective and powerful optimization methods. As a result, during the last three decades, researchers have been carrying out non-traditional optimization techniques like Ant Colony Optimization (ACO) [Yaseen and AL-Slamy, 2008] which works on the principle of foraging behavior of the ant for the food; Artificial Immune Algorithms (AIA) [DasGupta, 2014] based on the principle of human being's immune system; Genetic Algorithm (GA) [Michalewicz, 1996] based on the Darwinian theory principle of the survival-of-the fittest and the living beings' evolution theory; Differ-

ential Evolution (DE) [Price et al., 2006] which is similar to GA with a specialized crossover and selection method.

In this work, we will focus our attention in the stochastic (non-traditional) technique called Differential Evolution which will help us solving the inverse problem defined in Section 2.1.2.

3.1 General optimization definitions

Some general optimization definitions need to be done in order to understand future specifications about the subject treated in this work.

- Objective function: it is the function to be optimized by the optimization algorithm. Depending on the problem definition, it is proposed to maximize or minimize this function. As our desire in this work is to minimize, then, we will use it to make all the following definitions.

A generic nonlinear optimization problem with continuous variables is formulated as:

$$\begin{aligned} & \underset{x}{\text{minimize}} && f(\mathbf{x}) \\ & \text{subject to} && g_i(\mathbf{x}) \leq 0, \quad i = 1, \dots, m \\ & && h_i(\mathbf{x}) = 0, \quad i = 1, \dots, l \quad \mathbf{x} \in X, \end{aligned}$$

where f (objective function), g_1, \dots, g_m (inequality constraint), h_1, \dots, h_l (equality constraint) are functions defined on \mathbb{R}^n , X is the search space (a subset of \mathbb{R}^n), and \mathbf{x} is a vector of n components (x_1, \dots, x_n) .

The target here is to find a feasible point $f(\mathbf{x}^*)$ such that $f(\mathbf{x}) \geq f(\mathbf{x}^*)$ for each feasible point \mathbf{x} where \mathbf{x}^* represents the optimal solution to the problem.

- Unimodal and Multimodal Function: the unimodal function is the one that only has one peak (maximum) or valley (minimum) in a given interval [Rao and Rao, 2009]. This means that it exists only one optimum in a certain region. Mathematically, a real function f is unimodal in the interval $[a, b]$ if there is a point $x^* \in [a, b]$ such that f is decreasing in $[a, x^*]$ and f is increasing in $[x^*, b]$. Thus, a unimodal function doesn't need to be continuous because the same principle is satisfied if it is discrete. On the other hand, a multimodal function is the one that have several valleys or peaks in a given interval (see Fig. 3.1).

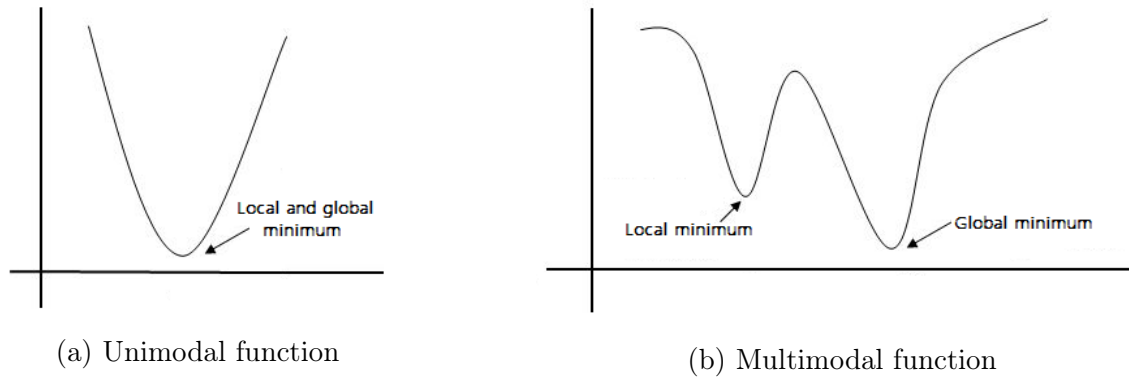


Figure 3.1: Local and Global minimums over unimodal and multimodal functions

- Optimality criteria: a function $f(x)$, defined over a set S , reaches a global minimum in $x^{**} \subset S$ if Eq. 3.1 is satisfied and it will reach a local or relative minimum in $x^* \subset S$ if Eq. 3.2 is satisfied.

$$f(x^{**}) \leq f(x), \quad \text{for all } x \text{ of } S \quad (3.1)$$

$$f(x^*) \leq f(x), \quad \text{for all } x \text{ of a distance } \varepsilon \text{ from } x^* \quad (3.2)$$

In other words, for Eq. 3.2, there is $\varepsilon > 0$, such as for all x satisfying $|x - x^*| < \varepsilon \rightarrow f(x^*) \leq f(x)$.

If a function is unimodal, the local minimum will be transformed automatically into a global minimum. When it is not, it has multiple local minimum so the global minimum will be reached only localizing all local minimum and selecting the better one (the one which minimizes $f(x)$). In Fig. 3.1 it is also shown the minimum points for both unimodal and multimodal functions.

3.2 Differential Evolution Algorithm (DE)

This algorithm was proposed by Rainer Storn and Kenneth Price [Storn and Price, 1995] for minimizing possibly nonlinear and non-differentiable continuous space functions. On this way, there are many researches addressing its use and the benefits that can be obtained implementing it.

An overview of Differential Evolution-based approaches used in electromagnetics was addressed in [Rocca et al., 2011]. This study pointed out the novelties and

customizations with respect to other fields of application. Also, it was presented a wide DE coverage used for solving electromagnetic optimization problems focused on antenna synthesis and inverse scattering, giving, in this way, the latest progress in this field. The conclusions of the study showed that Differential Evolution represents a reliable and effective alternative method to be carefully considered when approaching an optimization problem in electromagnetics. It was said that Differential Evolution cannot be stated as better than other evolutionary algorithms because of the "no free lunch theorem", but it generally outperforms other approaches dealing with small-scale optimization of continuous variables and it gives the possibility of introducing physical constraints or a priori knowledge about the problem at hand in a simple way.

Furthermore, diverse investigations have been performed with the purpose of comparing different optimization techniques and establishing what is the one that have better performance or applicability in different research fields. In this matter, the study [Vesterstrøm and Thomsen, 2004] evaluated the Differential Evolution, the Particle Swarm Optimization (PSO) and Evolutionary Algorithms (EA) on 34 widely used Numerical Benchmark Problems. This survey made it possible to examine which algorithm outperformed others in most of tested problems and also attempted to know particular difficulties or preferences of each one. Results showed that DE generally outperforms the other algorithms. It was more efficient and robust (by means of reproducing the results in several runs) than PSO and EA. Also, DE converges faster, finds the optimum in almost every run, has fewer parameters to set, and the same settings can be used for many different problems. This proved that DE is a good algorithm to solve numerical problems with real-valued parameters. However, in two noisy functions, Differential Evolution was outperformed by the Evolutionary Algorithms. This indicates further studies in this aspect that needs to be encouraged.

In [Qing, 2003], Qing used the DE algorithm in order to solve an inverse problem which consisted on locating, identifying, and recognizing two-dimensional perfectly conducting objects. Also, it was establish a comparison of the differential evolution strategy with the real-coded genetic algorithm, which was already studied for the same problem. Satisfactory results were obtained which fully demonstrate the features of the DE (search ability, simplicity, robustness). Furthermore, it was concluded that the DE outperforms the real-coded genetic algorithm for this kind of problem.

In other research [Qing, 2006], it was compared the DE strategy with a novel evolutionary algorithm called Dynamic Differential Evolution (DDE). The difference between this two similar techniques, lies in the population updating. DE updates its population generation by generation while DDE, as its name pointed, does it dynamically. These algorithms were tested on trial functions to be minimized, one with a

unique minimum and other with multiple minima. It was also analyzed in solving a benchmark electromagnetic inverse scattering problem. Results demonstrated that the dynamic differential evolution strategy significantly outperforms the differential evolution strategy in efficiency, robustness, and memory requirement. Besides this, using dynamic updating of population led to a larger virtual population size and quicker response to change of optimal search direction.

After this state-of-the-art, it has been evidenced that the DE can provide a good alternative to solve inverse problems related with geophysics, since surveys done about DE demonstrated it is a robust and easy to use algorithm [Price and Storn, 1997].

3.2.1 Method Description

There are three basic parameters of control in DE algorithm:

1. Population size N
2. Mutation constant F
3. Crossover constant Cr

Other parameters to take into account are: number of generations G (stop criteria), upper and lower boundary constraints and problem dimension S .

The DE method starts generating a random population equals to the N defined by the user. This population would represent the problem's initial solution. Then, using Eq. (3.3) a mutant vector V_i is generated using three different target vectors randomly selected previously.

$$V_i = R_{1i} + F(R_{2i} - R_{3i}) \quad i = 1, 2, 3, \dots, N \quad (3.3)$$

The random target vectors are represented by R_{1i}, R_{2i}, R_{3i} . R_{1i} is called base vector and the second term of the equation is a weighted difference of two target vectors. The mutation constant F is defined by the user, and its optimal value ranges between 0.4 and 1 [Price and Storn, 1997].

Then, from the target and mutant vector, it's obtained a new trial vector U_i based on the crossover probability Cr . This Cr constant controls the quantity of values to be inherited by U_i from the mutant vector. If $Cr = 1$, the trial vector will be equal to the mutant one. Later, the trial vector and the current target one are compared in order to choose the best of them for next generation.

In summary, the general operations of the Differential Evolution method are presented in Fig. 3.2.

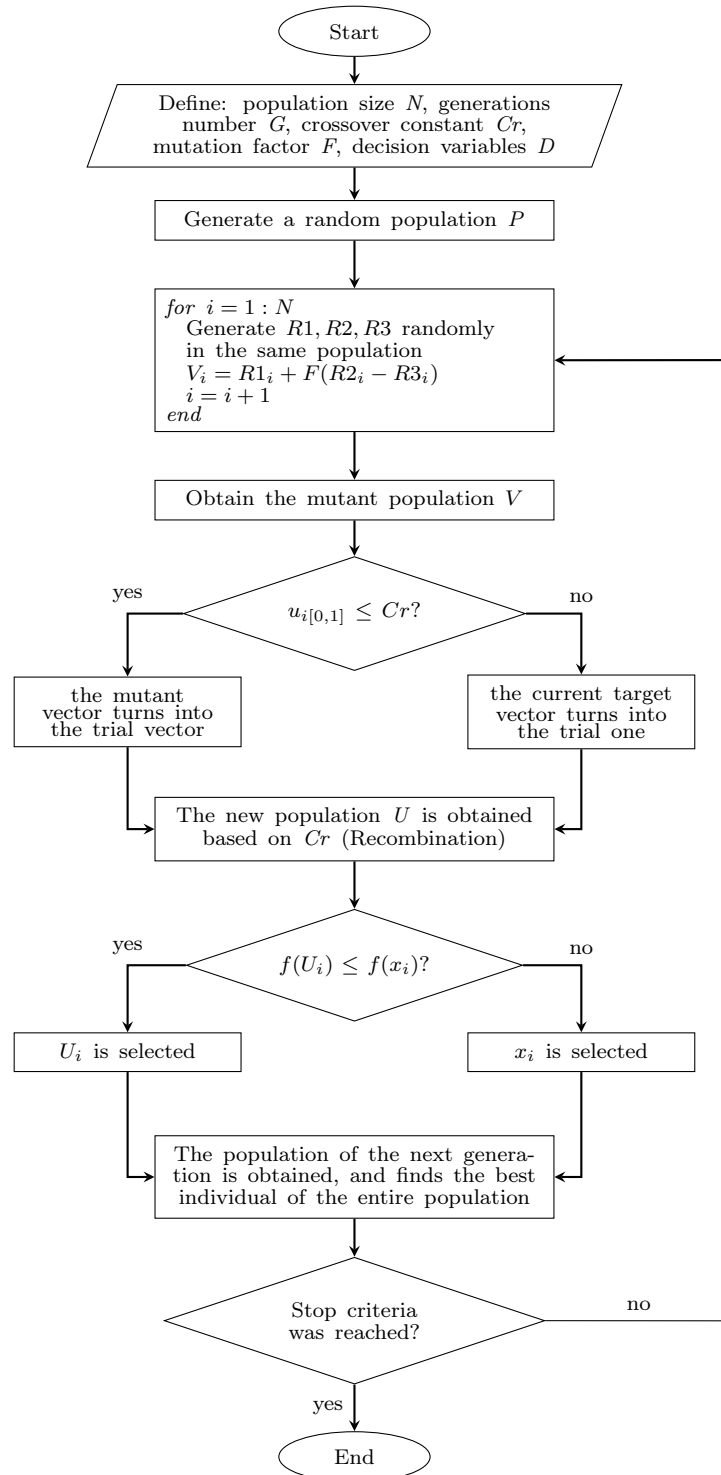


Figure 3.2: Flowchart of the differential evolution algorithm

3.3 Inverse Pavement problem

In broad terms, an inverse pavement problem can be defined as an optimization problem as follows

$$\begin{aligned} & \underset{x}{\text{minimize}} && f(\mathbf{x}) \\ & \text{subject to} && \underline{x}_i \leq \mathbf{x}_i \leq \bar{x}_i, \quad i = 1, \dots, m \end{aligned}$$

where \underline{x}_i and \bar{x}_i are the vectors of minimum and maximum values, respectively, presented previously for typical pavement materials in Table 2.1.

$f(x)$ is the quadratic error function, which represents the forward problem, defined as

$$f(x) = |E_{GPR} - E_r(\mathbf{x})|^2$$

E_{GPR} symbolizes the reflected electric field measured with the GPR, $E_r(\mathbf{x})$ represents the reflected electric field obtained in the forward problem, analytically or using some numerical method, for \mathbf{x} , which represents the solutions vector, for n layers, in this way:

$$\mathbf{x} = [\epsilon_1, d_1, \epsilon_2, d_2, \dots, \epsilon_n, d_n]$$

3.3.1 The reference problem

As it was already mentioned, the objective function to be analyzed in this work is a function of the measured reflected electric fields by the GPR.

Therefore, we selected a representative problem, defined constants within the range of typical values, and they were considered as such measurements or reference. These values were randomly selected between the ranges consigned in Table 2.1. In order to specify the selected reference parameters, they were arranged in Table 3.1. These quantities, at the end, will be the ones to be found by the optimization algorithm as optimum values (x^*). So, $x^* = [6, 8, 5.5, 25, 10]$.

Layer	$\epsilon_{r_{ref}}$ (F/m)	d_{ref} (cm)
1. Asphalt	6	8
2. Base	5.5	25
3. Sub-grade	10	—

Table 3.1: Pavement materials pavement selected as reference

Chapter 4

Approach Methods and Results

In order to evaluate the methods, we tested them on flexible pavement structure as shown in Section 2.2.1. Therefore, this chapter aims to highlight the advantages and disadvantages of using different techniques in the assessment of pavement properties using the GPR. First, we present results of the time domain approach proposed in [Loizos and Plati, 2007] where the travel time and amplitude of reflective signal are used to obtain the roads characteristics. Then, the frequency domain method is analyzed using the methodology described in [Oliveira et al., 2014]. It basically intends to analyze the error function establishing a maximum GPR operation frequency to guarantee an objective function with a global minimum. A third methodology is defined as our proposal. This is similar to the one defined by [Oliveira et al., 2014] but we expanded the error function to include a frequency band. Results of the third approach are summarized in [Africano and Adriano, 2014]. The simulations of the three approach methods were implemented in *MATLAB* using the Finite Difference Time Domain (FDTD) for the forward problem in time domain and the analytical solution for frequency domain (See Section 2.1.1).

4.1 Time Domain approach

One possibility for solving the inverse problem is described in [Loizos and Plati, 2007]. It proposes to use the reflected signal in time domain to take some information about it (wave amplitude and travel time). Then, using this information, it determines the dielectric constant of each layer through the amplitudes of the reflected pulses collected by an air-coupled GPR system. Once the dielectric properties are obtained, the thickness of each layer is obtained using the travel time information.

To reproduce the methodology of this time domain approach, the reference prob-

lem was simulated using the FDTD technique. To accomplish this, an incident wave was generated by using a current source which produced a Gaussian pulse (J_z) defined as

$$J_z(t) = e^{-\frac{(t-t_0)^2}{\tau^2}} \quad (4.1)$$

where t_0 is the amount of the time shift chosen as $\sqrt{20}\tau$ and τ is the parameter that determines the width of the Gaussian pulse. This can be known using Eq. (4.2). On it, f_{max} is the highest frequency that is available out of an FDTD calculation.

$$\tau = \frac{\sqrt{2.3}}{\pi f_{max}} \quad (4.2)$$

As a result of the FDTD simulation, the reflected electric field measured at the GPR receiver is presented in Fig. 4.1. The trace main peaks (A_1 , A_2 and A_3) represent the impact of the incident wave on each interface.

Once the reflected electric field wave is achieved, the dielectric value of the asphalt pavement course (first layer) can be calculated using Eq. (4.3). Where A_1 is the reflection amplitude generated right after the wave pass from one medium to another, in this case, from the air to the asphalt layer. A_m represents the amplitude of the

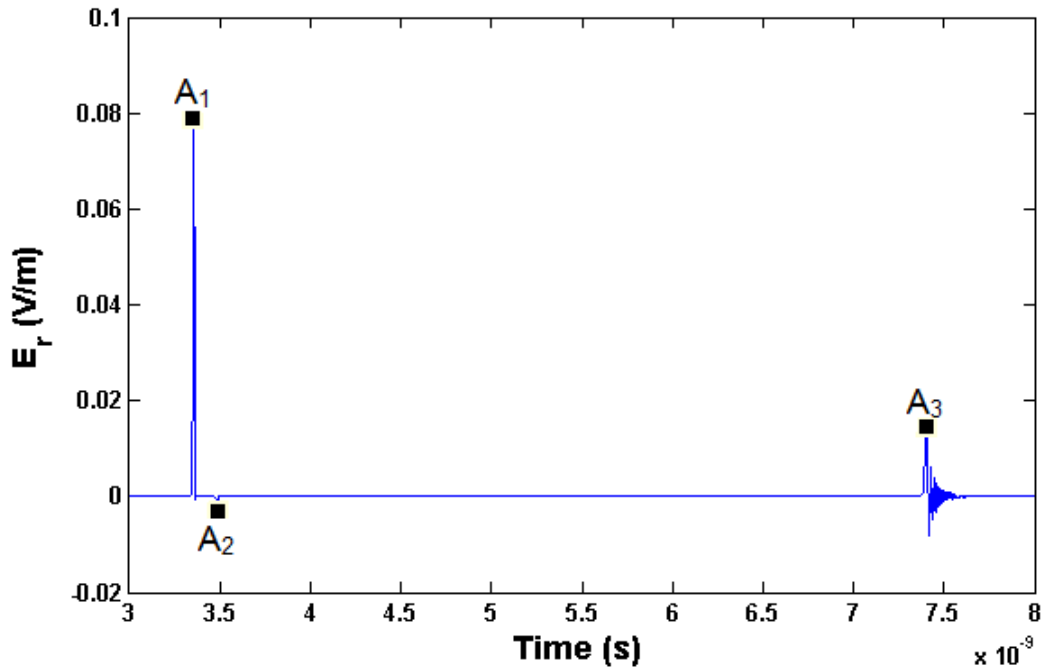


Figure 4.1: GPR trace simulated using FDTD method at 9 GHz

inverse incident GPR signal. This amplitude is measured during the GPR calibration process using a large metal plate placed on the pavement surface. Therefore, this measured signal can be assumed to be the inverse incident GPR signal since metal is considered a perfect conductor and, thus, an electromagnetic reflector that will cause the wave to be completely reflected.

$$A_1 = -A_m \cdot \Gamma_1 \quad (4.3)$$

Finally, Γ_1 is the reflection coefficient of interface 1 defined as

$$\Gamma_1 = \frac{\eta_1 - \eta_0}{\eta_1 + \eta_0} = \frac{\sqrt{\mu_r/\epsilon_{r1}} - 1}{\sqrt{\mu_r/\epsilon_{r1}} + 1} = \frac{1 - \sqrt{\epsilon_{r1}}}{1 + \sqrt{\epsilon_{r1}}} \quad (4.4)$$

where η represents the intrinsic medium impedance, μ_r and ϵ_{r1} are the medium permeability and permittivity, respectively.

As we can see on Eq. (4.4), the reflection coefficient is in function of the medium permittivity. So, when it is substituted in Eq. (4.3), we can isolate the permittivity, leaving it as a function of the known amplitudes as specified in Eq. (4.5).

$$\epsilon_1 = \left(\frac{1 + \left(\frac{A_1}{A_m}\right)}{1 - \left(\frac{A_1}{A_m}\right)} \right)^2 \quad (4.5)$$

The same procedure is handled for the estimation of the dielectric constant to subsequent layers. Then, from Eq. (4.6) and Eq. (4.7), the permittivity for layer 2 and 3 is obtained respectively as described in Eq. (4.8) and Eq. (4.9).

$$\sqrt{A_2} = A_{inc} T_{01} \Gamma_2 T_{10} \quad (4.6)$$

$$\sqrt{A_3} = A_{inc} T_{01} T_{12} \Gamma_3 T_{21} T_{10} \quad (4.7)$$

where T_{01} , T_{12} , T_{10} , and T_{21} are the transmission coefficients from air to layer 1, layer 1 to layer 2, layer 1 to air and from layer 2 to 1, respectively. Γ_2 and Γ_3 are the reflection coefficient of layer 1 to layer 2 and layer 2 to layer 3 interfaces.

$$\sqrt{\epsilon_2} = \sqrt{\epsilon_1} \left(\frac{1 + \left(\frac{A_2 A_m}{(A_m - A_1)(A_m + A_1)}\right)}{1 - \left(\frac{A_2 A_m}{(A_m - A_1)(A_m + A_1)}\right)} \right) \quad (4.8)$$

$$\sqrt{\epsilon_3} = \sqrt{\epsilon_2} \left(\frac{A_2 - A_2\Gamma_2^2 - A_3\Gamma_2}{A_2 - A_2\Gamma_2^2 + A_3\Gamma_2} \right) \quad (4.9)$$

Now, for layers thickness estimation, the travel time of the transmitted pulse within a pavement layer is used, along with the dielectric properties of the studied layer obtained using Eqs. (4.5) (4.8) (4.9). Since materials frequently used in GPR studies are considered of low loss, the wave propagation velocity (v_L) can be expressed for each layer by Eq. (4.10). From this equation, it is possible to isolate the thickness for any layer (d_L) and, then, to compute it according to Eq. (4.11).

$$v_L = \frac{c}{\sqrt{\epsilon_{rL}}} = \frac{2d_L}{\Delta t_L} \quad (4.10)$$

$$d_L = \frac{c}{\sqrt{\epsilon_{rL}}} \cdot \frac{\Delta t_L}{2} \quad (4.11)$$

On this equations, c is the velocity of light, ϵ_{rL} represents the permittivity of each layer $L = [1, 2, \dots, L_{max}]$ and Δt_L is the time delay between the peak from the layer under study and the next one. For example, for layer 1, $\Delta t_L \rightarrow \Delta t_1$ and it will be the time delay since peak A_1 to peak A_2 in Fig. 4.1.

This time domain analysis was applied in the pavement structure selected defined in section 2.2.1. The computed values using this procedure are consigned in Table 4.1. In it, it is also specified the quadratic error percentage for each estimated variable with respect to the reference. After a comparison between the obtained quantities and the reference ones showed in the table, it is possible to conclude that the parameters (permittivity and thickness) of the pavement layers were almost properly obtained by using the time domain approach proposed in [Loizos and Plati, 2007]. Also, it is important to emphasize in the cascading error presence, i.e, this method brings an increasing error after each calculation.

There are two main drawbacks about this method that it is necessary to take

	Variable	Obtained value	Error (%)
Asphalt layer	ϵ_1	5.919	0.1
	d_1	0.081 m	0.00125
Base layer	ϵ_2	5.441	0.1
	d_2	2.518 m	2057.53
Subgrade layer (soil)	ϵ_3	7.936	42.6
	d_3	—	—

Table 4.1: Results using time domain approach

into account because these will make the adequate detection of the reflected peaks a difficult task.

One disadvantage is based on how the reflections can be affected by the width of the incident pulse. To explain this, it is important to mention the concept of resolution, a very important issue of GPR studies. For GPR pavement analysis, vertical resolution provides a significant information about the ability that the equipment has to discriminate layers in the subsoil by the thickness. Here, there is a close relation between pulse width, frequency and thickness of the medium under evaluation. Typically, pulse width is constituted by $1\frac{1}{2}$ - 2 times the nominal frequency of the antenna characteristic [Biskup et al., 2005]. Its short duration in time domain (Δt) is associated with an increase inversely proportional to the contribution of its frequency components (Δf) according to $\Delta t = 1/\Delta f$ relation. So, pulse width, in principle, decreases as the frequency increases. Therefore, working with a low frequency will affect the method effectiveness if this has a very thin layer because it will generate overlapping of the peaks amplitudes. Thereby, it complicates the proper association of the reflected pulses with the corresponding interface where reflection originates.

Fig. 4.2 attempts to illustrate this pulse width effect over the entire pavement using a smaller frequency (1 GHz) than the presented in Fig. 4.1. In order to evidence the specific variation of using difference frequencies and visualize the effect of it, an expanded view of the first two peaks, which are generated from the interfaces of the finest layer (for this work, of 8 cm), is shown in Fig. 4.3. As depicted, the simulation at 9 GHz allowed to obtain results with good resolution and, therefore, reflected pulses are clearly defined compared to the ones obtained later in the simulation at 1 GHz. It is possible to see that, for 1 GHz, the peaks start to overlap one on another and, thus, it implies a bigger effort to perform their automatic detection.

Another significant drawback of the method is that noise may appear on real GPR measurements adding more complexity to the detection process. Fig. 4.4 depicts the reflected pulses obtained with a noise signal. The noise signal type added to the original signal was a white random noise of 1 percent. Table 4.2 contains the achieved parameters of the method for GPR measurements with noise and the percentage quadratic error of the results. It is proved, then, that when noise appears over the signal, the pulses amplitude estimation is much more difficult.

To sum up, after the method analysis, it was determined that it is a good choice to estimate the pavement parameters but its accuracy is highly dependent on the evaluation of the reflection instants, the peak amplitudes and the pulse frequency or pulse width. The presence of multiple reflections worsens the method performance, since it is difficult to associate the reflected pulse to its respective interface where

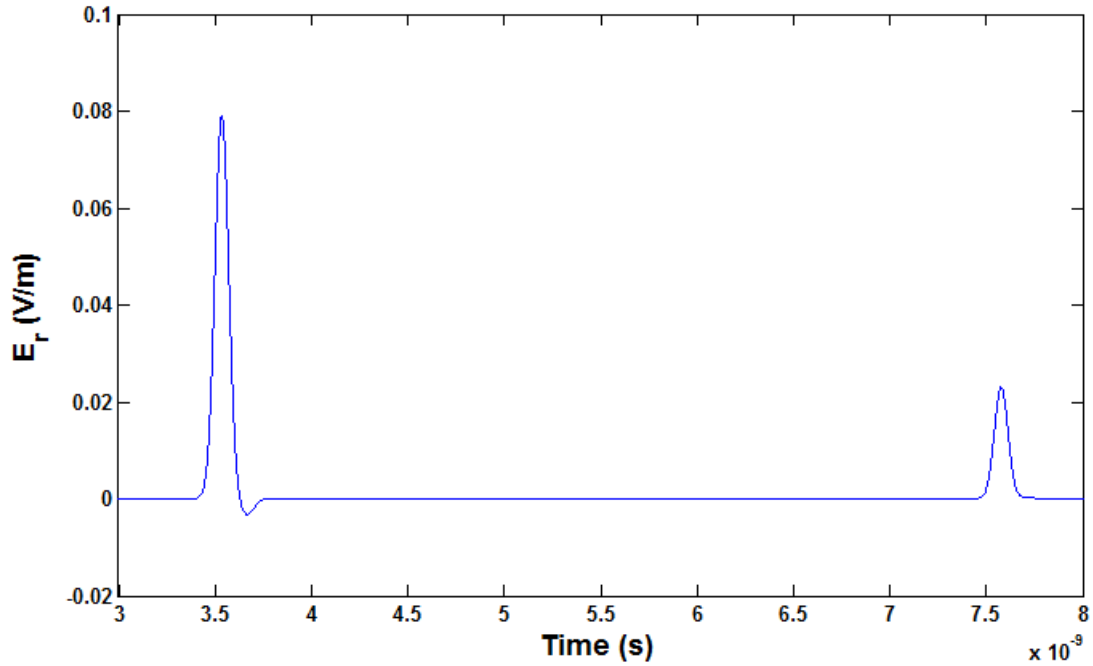
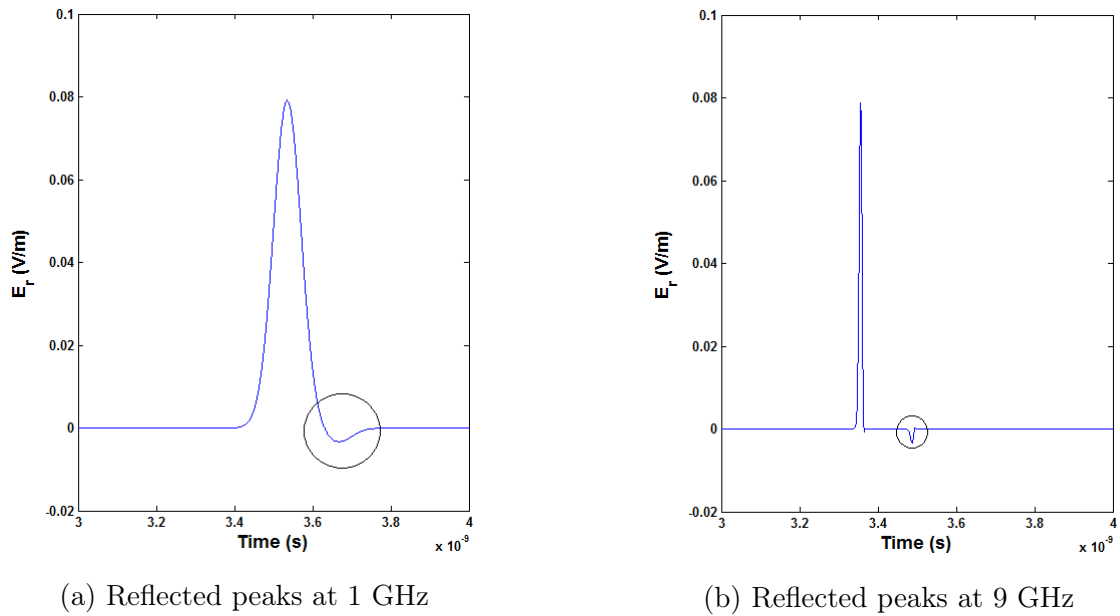


Figure 4.2: GPR trace simulated using FDTD method at 1 GHz



(a) Reflected peaks at 1 GHz

(b) Reflected peaks at 9 GHz

Figure 4.3: Electric reflected field pulses at two different frequencies

it was originated. Moreover, very thin layers generate overlapped pulses that are not obtained easily and this will generate a cascading error which means that the quadratic error is going to propagate over each estimation.

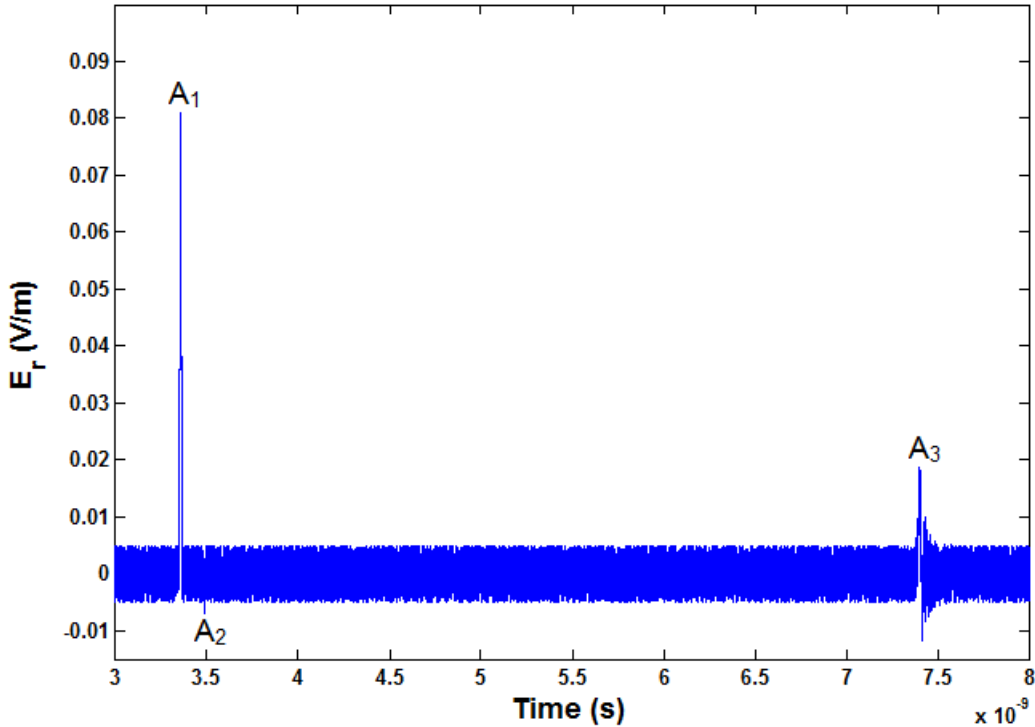


Figure 4.4: GPR measurement adding random noise

	Variable	Obtained value	Error (%)
Asphalt layer	ϵ_1	6.704	8.272
	d_1	0.076 m	0.016
Base layer	ϵ_2	5.468	0.02
	d_2	2.511 m	2045.38
Subgrade layer (soil)	ϵ_3	8.666	17.81
	d_3	—	—

Table 4.2: Percentage error values for GPR reflected electric field signal simulated with white random noise at 9 GHz

4.2 Frequency Domain approach

Another possibility to estimate the pavement parameters is by using a frequency domain analysis. In this case, the characteristics of the multiple layers cannot be obtained in a closed form. The problem is generally presented as an electromagnetic inverse problem, which is usually solved using some optimization method. Given the nature of the problem, constraints must be imposed to ensure the solution uniqueness [Tarantola, 2005].

A frequency domain methodology for the GPR multilayer problem is presented in [Oliveira et al., 2014]. The article attempts to determine how the parameters,

permittivity, thickness, and frequency of the incident wave affect the posedness of the inverse problem. Also, it proposes a methodology to ensure the well-posedness of the problem taking into account the limits of the problem variables.

The propose of Oliveira *et al.* to solve the inverse problem is to minimize the quadratic error function defined as

$$erf = \|\mathbf{E}_r(\mathbf{d}, \boldsymbol{\epsilon}) - \mathbf{E}_{ref}\|^2 \quad (4.12)$$

where $\mathbf{E}_r(\mathbf{d}, \boldsymbol{\epsilon})$ is the predicted reflected field computed using the same mathematical model to the one defined in 2.1.1 for one frequency value. $\mathbf{d} = [d_1, \dots, d_L]$ and $\boldsymbol{\epsilon} = [\epsilon_1, \dots, \epsilon_L]$ represent the thickness and permittivity, respectively, of the L composing layers. Finally, \mathbf{E}_{ref} represents the measurements or the reference values.

However, it is highlighted in the article that minimizing the error function (4.12) will not guarantee the correct solution, given that the function generally represents a nonlinear and multimodal problem that can be ill-posed. In order to evidence this, the behavior of the error function was analyzed respecting the layer thickness and permittivity variables.

Error function and layer thickness relation

The variation of one layer thickness, maintaining the others pavement parameters as constants and one GPR frequency, influenced the error function to present the characteristics of an ill-posed problem. Fig. 4.5 shows this characteristic for the function. In this figure, we can observe the error/objective function represented with the blue line; the reference values, i.e, the measurements, represented by the red line and, finally, the computed predicted values denoted by the black line. As depicted, there is the presence of multiple global optimum in the objective function which demonstrates that the problem is ill-posed. Under these considerations, any algorithm that attempts to solve it may converge on wrong optimal solutions. With the purpose of overcoming this, it is proposed to make the problem well-posed employing the relation described by Eq. (4.14). With this, a maximum frequency is set for each layer knowing the limits of the thickness variables. After the maximum frequency for each layer is known, it is selected the lowest one to set up the GPR, ensuring this way, a unimodal error function in the vicinity of the optimum point.

$$\Delta d_i \leq \frac{1}{2} \lambda_{i, f_{max}} \quad (4.13)$$

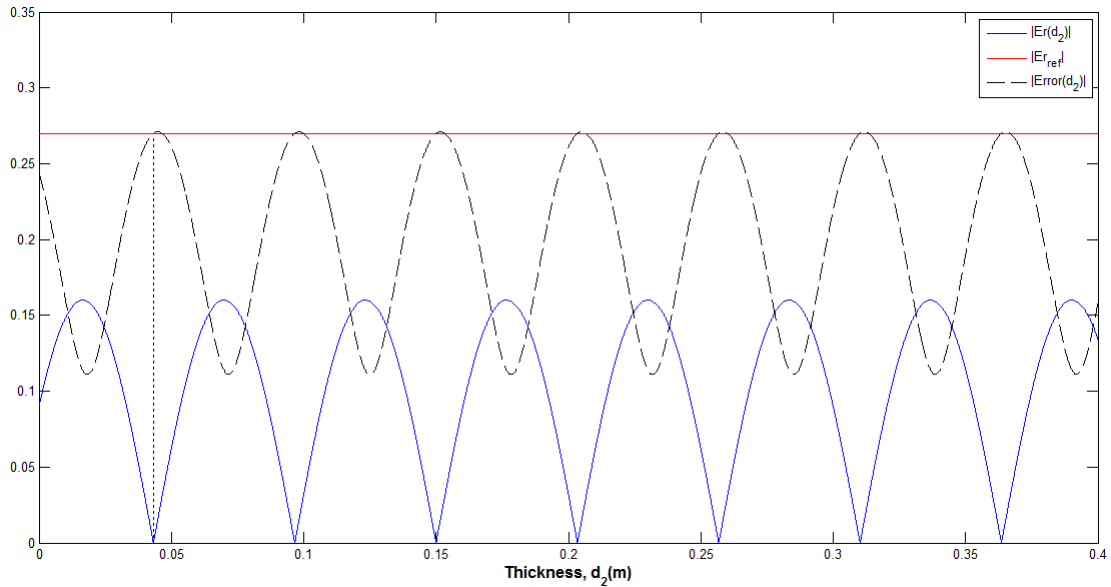


Figure 4.5: Error function and layer thickness relation

$$f_{max} \leq \frac{1}{2} \frac{1}{\sqrt{\mu_0 \epsilon_0}} \frac{1}{\sqrt{\epsilon_i}} \frac{1}{\Delta d_i} \quad (4.14)$$

where i represents the layer, Δd_i is the feasible deviation for each thickness variable, ϵ_i is the reference typical permittivity value in each layer i and μ_0 and ϵ_0 are the permeability and permittivity in the air respectively.

Error function and layer permittivity relation

On the other side, an analysis of changing permittivity values and frequencies in the error function was performed similarly to the previously done for thickness variations. So, all pavement parameters were maintained as constants except the permittivity of one layer. In this way, Fig. 4.6 was obtained to see the behavior of the error function for two frequencies selected (200 MHz and 1.5 GHz) and permittivity variations. It is possible to evidence that the error function has one global minimum in each frequency and its behavior becomes more oscillatory as the frequency increases.

To sum up, we realized, after this analysis, that it is possible to determinate a maximum frequency for the GPR incident wave that guarantees the well-posedness of the solution, considering that the range of the thickness of each layer is well-known. Additionally, defining the maximal frequency that ensured the uniqueness of the solution also results in a unimodal optimization problem. Consequently, deterministic optimization tools can be applied resulting in fast convergent methods.

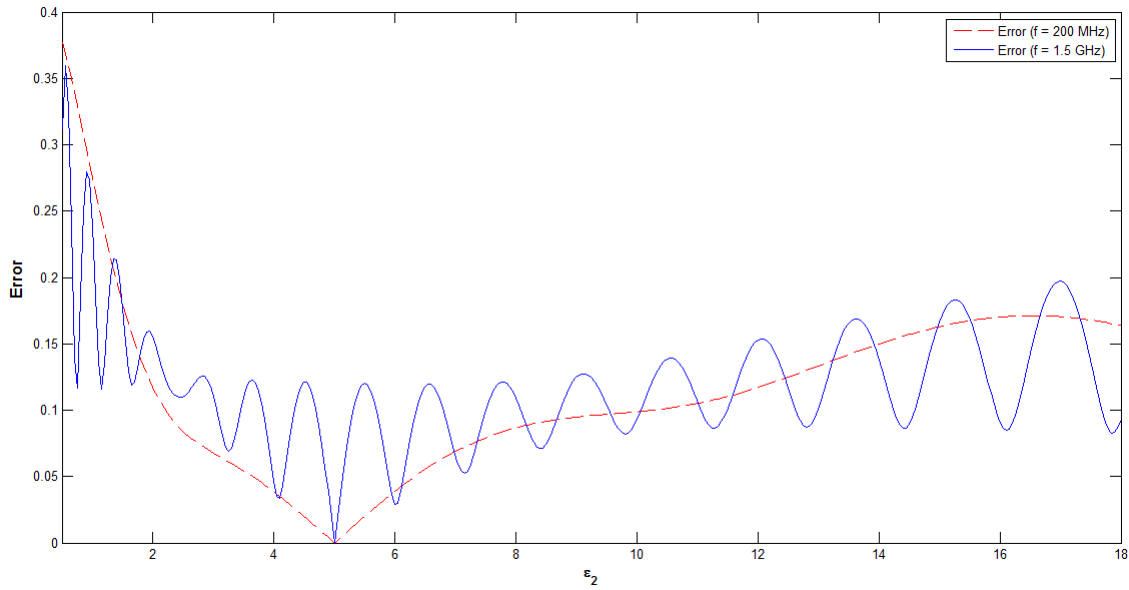


Figure 4.6: Error function and relative permittivity relation for 200 MHz and 1.5 GHz

Now, results of using this methodology are presented here. Employing the Eq. (4.14) presented by Oliveira *et al.* to the test problem described in section 2.2.1 allows us to obtain the frequency values for each layer (consigned in Table 4.3). Then, it is selected the one lowest to set it as the GPR frequency. In consequence, it was set a frequency value of approximately 600 MHz as maximum frequency. With this value it was simulated the objective function (Eq. (4.14)) for variation in the first layer parameters with the purpose of visualizing its behavior (Fig. 4.7). As depicted, the error function guarantees unicity using this maximum frequency showing only one global minimum, but it does not result in a unimodal optimization problem given that the feasible deviation of both pavement parameters is too large. We realize that this work is only valid to small perturbations. If pavement variables range is small, it is guaranteed a smooth function behavior, which means, a unimodal function around the optimum point. Therefore, we also show the behavior of this objective function for a lower frequency in order to observe the changes on it. In this way, the same procedure was applied but, this time, for a frequency of 200 MHz and the function characteristic is presented in Fig. 4.8. As we note, the function clearly has less variation, a smooth behavior and it has turned into a unimodal problem.

After obtaining these results, it is possible to conclude that for both GPR frequencies the objective of guaranteeing a well-posed problem was reached. Nevertheless, when this frequency is close to the limit frequency, the maximum proposed, its behavior starts to be multimodal, creating the necessity of taking into account just the vicinity

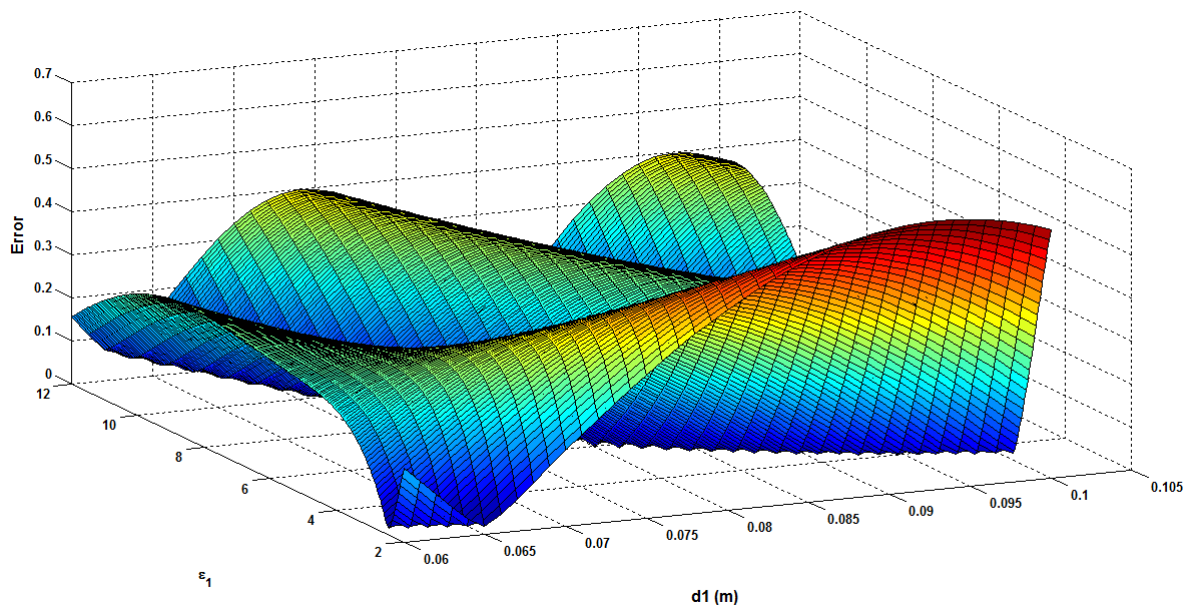


Figure 4.7: Error function vs. ϵ_1 and d_1 for the maximum frequency value (600 MHz)

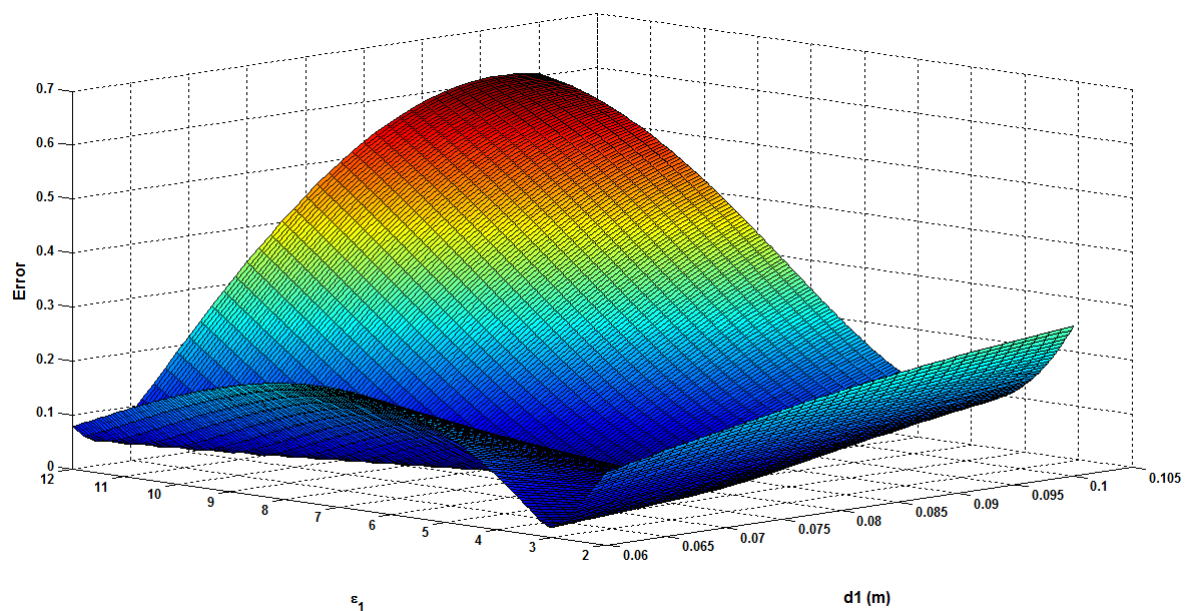


Figure 4.8: Error function vs. ϵ_1 and d_1 for a frequency value lower than maximum (200 MHz)

Layer	Δd (m)	ϵ_{ref}	f_{max} (Hz)
1. Asphalt	0.06 - 0.10	6	1.53×10^9
2. Base	0.2 - 0.3	5.5	611.95×10^6
3. Sub-grade	0.10 - 0.25	10	—

Table 4.3: Thickness limits, reference permittivity and computed maximum frequency

of the optimum point to guarantee the unimodality. Besides, selecting a lower value instead of the maximum one will also proportionate the unimodal characteristic which gives the benefit, in both cases, that the problem can be solved in a simple way by using a deterministic algorithm.

The main drawback concerning the existence of a maximal frequency is the size of the antenna. Setting a maximal frequency will limit the minimal size of the antenna which is an important aspect to take into account. To avoid this drawback, our propose, explained in detail in next section, attempts to modify the methodology presented in [Oliveira et al., 2014] to guarantee the well-posedness of the problem without the maximal frequency restriction.

Another possibility presented in the article to guarantee a well-posed problem consists on using two different frequencies (1 GHz, 1.5 GHz) to excite the pavement structure, instead of nly one GPR frequency. Then, its respective error function ($Error_1$, $Error_2$) is calculated and plotted for thickness variations as shown in Fig. 4.9. Given that, each error function has different period, the sum of them brings that the function

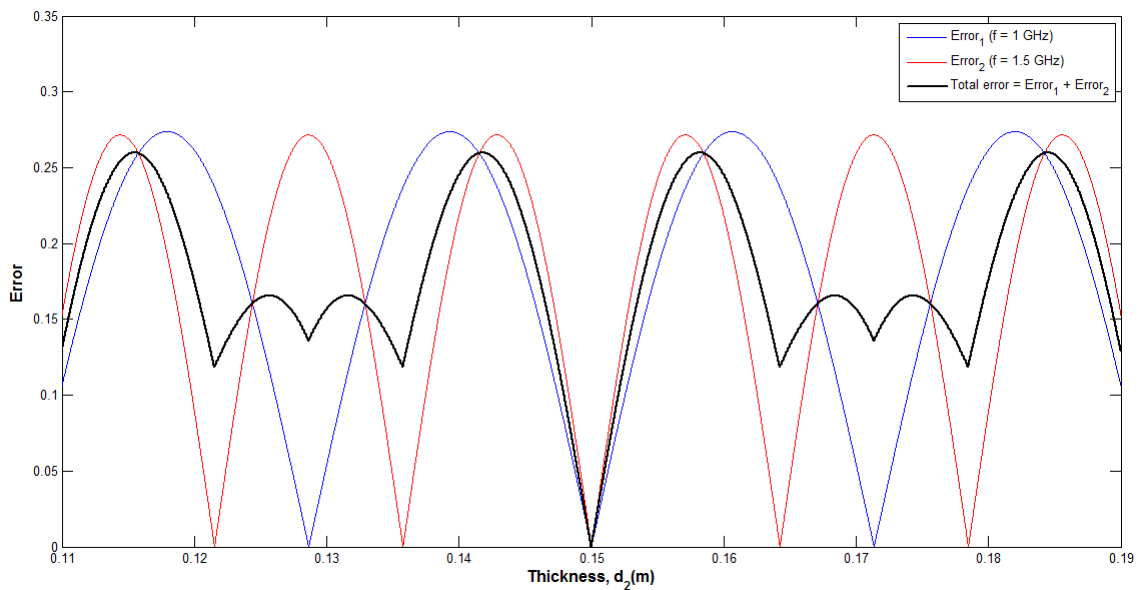


Figure 4.9: Error function and layer thickness relation for two different GPR frequencies

(4.12) becomes a well-posed problem with only one global minimum as depicted in Fig. 4.9 with the black line. Nevertheless, the article does not discuss ways to solve this multimodal system which has the presence of multiple local minimums. It also does not explore the effect of this in the search space. Consequently, our propose intends to perform a deeper analysis on the matter.

4.3 Multiple frequency approach

In this part of the work it will be described another approach that aims to take advantage of the two methods already mentioned. Since this method can be extracted from a pulse that is usually used in the time domain and uses all the frequency domain analysis to obtain the results. We suggest to base the inverse problem on the error function analysis where GPR data is compared with the computational one. It is important to highlight that the objective function proposed is similar to the one defined in [Oliveira et al., 2014]. But, we expanded it to include a frequency band.

Essentially, this proposal allows us to achieve the relaxation of the problem analyzing the error function by using a frequency summation. In this way, the new objective function can be described as

$$Error = \sqrt{\sum_{f_{min}}^{f_{max}} \frac{(\mathbf{E}_{GPR}(f) - \mathbf{E}_C(f))^2}{n}} \quad (4.15)$$

where $\mathbf{E}_{GPR}(f)$ is the value of GPR reflected electric field of reference, $f_{min} - f_{max}$ are the minimum and maximum frequency used in the selected frequency band, respectively, and n is the length of the frequency vector. Now, $\mathbf{E}_C(f)$ represents the value of the computed reflected electric field which was estimated using the electromagnetic direct problem presented in section 2.1.1. It is possible to realize that this function will depend on GPR frequency and thickness and permittivity values. For this study, the $\mathbf{E}_{GPR}(f)$ value is also computed by using the analytical expression defined on section 2.1.1 and the parameters defined in Table 3.1.

An analysis of the error function, when thickness and permittivity vary, enable us to verify if the relaxation of the inverse problem occurs for the frequency summation proposed in Eq. (4.15). Therefore, the error function was simulated varying according to the frequency band, the permittivity and the thickness of the first layer using the Eq. (4.15). The other layers' values of dielectric constants and thickness were defined as constants (according to Table 3.1) just in order to visualize the characteristic of the

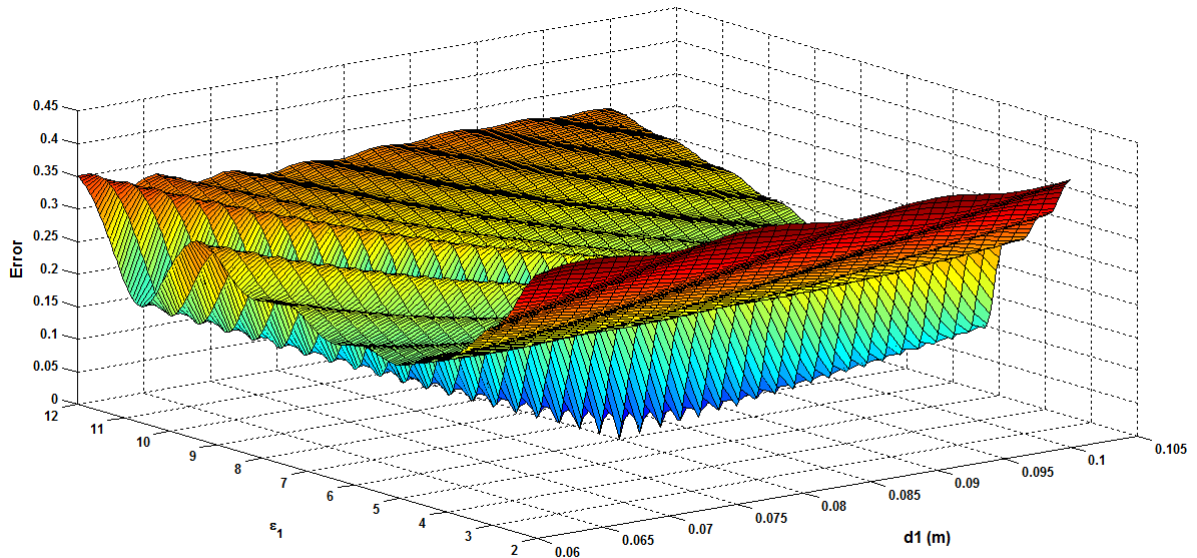


Figure 4.10: Error function vs. ϵ_1 and d_1 for a frequency summation (500 MHz - 2.5 GHz)

function. The frequency range was defined as $f_{min} = 500MHz$; $f_{max} = 2.5GHz$.

The function behavior is presented in Fig. 4.10. In this figure, we can observe that the problem continues well-posed for our proposal, i.e., the solution to this problem is a single solution guaranteeing, of this way, uniqueness. Also, it is possible to see that the problem has a strong multimodal characteristic. This characteristic represents a difficulty to solve the inverse problem with deterministic optimization tools. Nevertheless, there are stochastic algorithms that can help with this kind of problem (some of these were already mentioned in chapter 3).

The minimizing problem (4.15) was solved using the Differential Evolution algorithm (DE) described in section 3.2. We performed three different tests, taking into account all variables ranges presented in Table 2.1. For the tests, the stop criterion selected was an error coefficient that equals to 0.001. However, if the defined number of generations is achieved, the program will also stop the execution.

4.3.1 Optimization of the first layer

The objective of carrying out this test was to find the pavement parameters, permittivity and thickness, for the asphalt layer (layer 1). Therefore, we considered the frequency summation from 500 MHz to 2.5GHz. For the parameters of control defined for DE algorithm, we selected a population size $N = 120$, a mutation constant $F = 1$ and a crossover constant $Cr = 0.8$. Also, as input it was chosen a maximum number

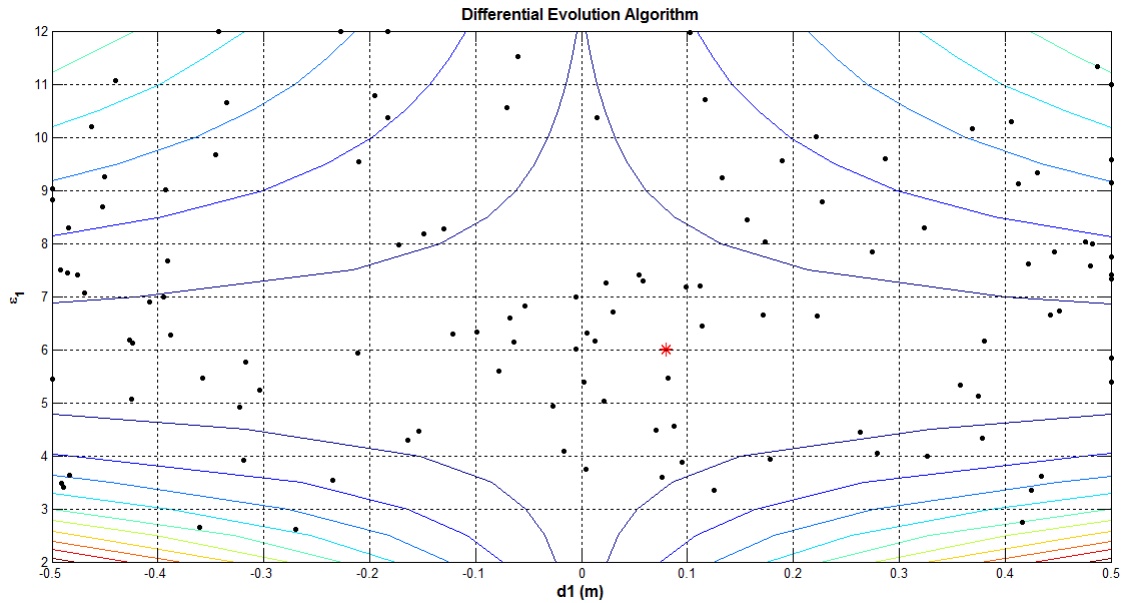


Figure 4.11: Level curves and best estimated value of two variables for a frequency summation with $f_c = 1.5GHz$

of iterations (generation) equals to 200.

The Fig.4.11 depicts the level curves, the initial population (represented by black points), and the best estimated value for the layer 1 (represented by the red star) which was selected as the problem solution. Then, the Fig.4.12 presents the evolution of the error function according to the generations. The algorithm finalized when it reached the set value for the error coefficient with a generation number equals to 98. As we can see, the objective function is decreasing in each generation and the number of generations is small for the problem nature. The obtained pavement values after compiling the program were 0.08 m for thickness and ϵ_r equals to 6 for the permittivity of asphalt layer. After obtaining this parameters, they were compared with the reference ones and they match with the reference problem.

4.3.2 Complete problem

The second test was conducted to find the characteristic parameters of a flexible pavement structure as shown in Fig. 2.5. In this way, the number of pavement variables or parameters to obtain increased to 5.

Just as in test 1, here, it was considered the error function (4.15) as objective function, the reference values in Table 3.1, the frequency summation from 500 MHz to 2.5GHz. Also, for DE parameters, the mutation factor was kept as 1 and the crossover constant as 0.8. However, the maximum number of iterations (generations)

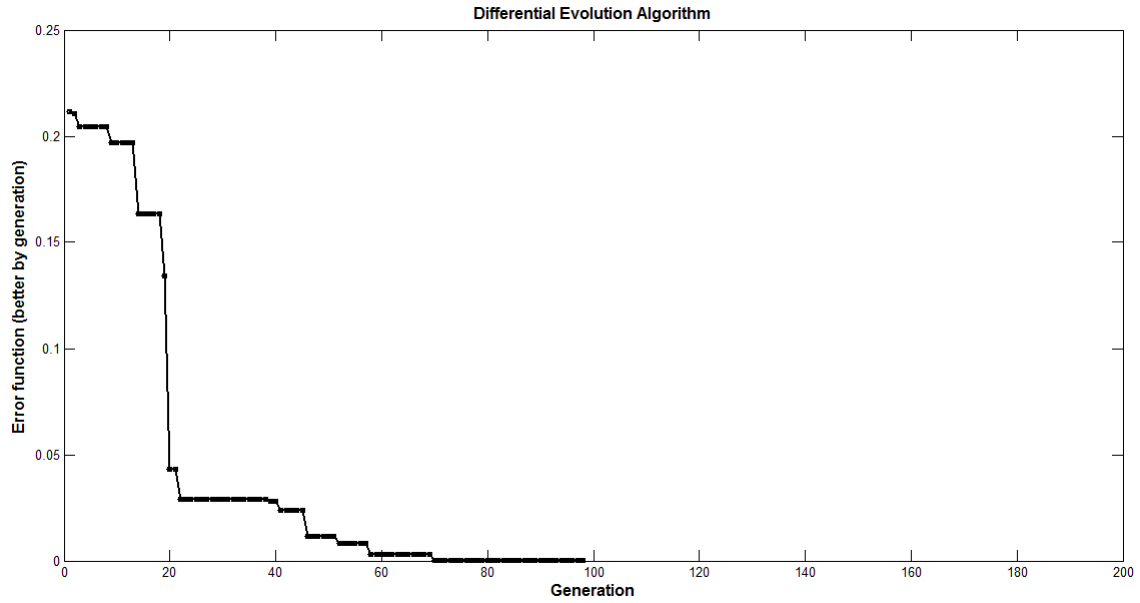


Figure 4.12: Better error function by generation for two variables using a frequency summation with $f_c = 1.5GHz$

was increased to 1000 and the initial population set as 480.

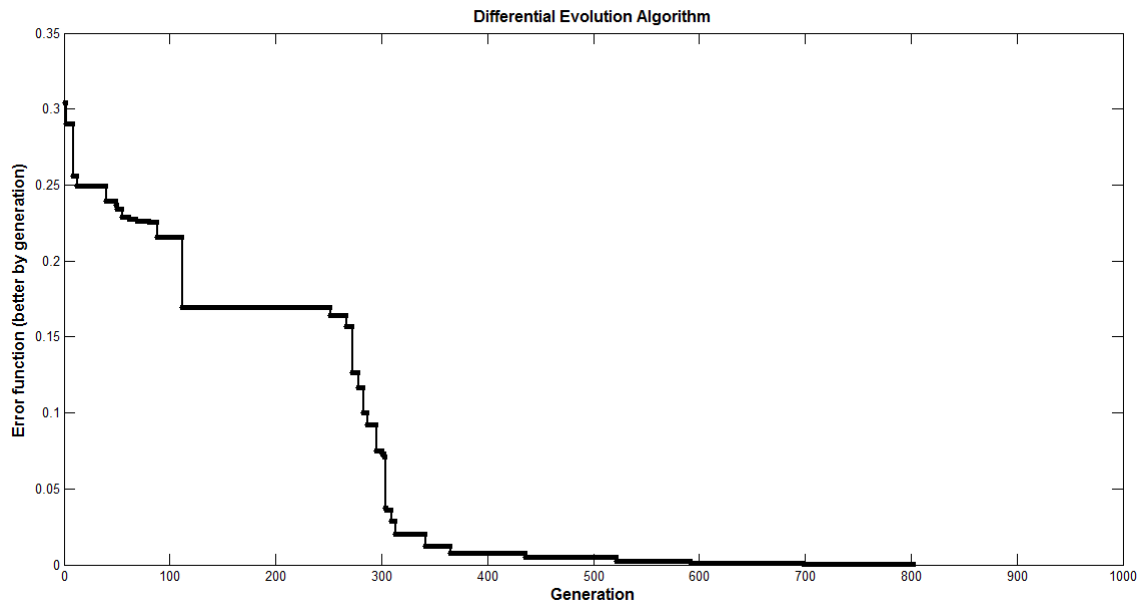
After the algorithm execution, Fig.4.13 was obtained. There, the evolution of the error function with each generation for the three layers case is shown. The results achieved by the algorithm in test 2 are presented in Table 4.4. In this instance, the maximum number of iterations was not reached ($g=802$). Thus, the program stopped when the error coefficient found was 0.001. Given these results, we considered the solution of the inverse problem satisfactory since results of pavement values matched with the reference ones (See Table 4.5).

	Layer	ϵ_r (F/m)	d (m)
Reference Model	1. Asphalt	6	0.08
	2. Base	5.5	0.25
	3. Subgrade (soil)	10	—
Algorithm	1. Asphalt	6.0005	0.0800
	2. Base	5.5008	0.2499
	3. Subgrade (soil)	10.0000	—

Table 4.4: Reference model and algorithm results

	Variable	Error (%)
Asphalt layer	ϵ_1	0.04e-4
	d_1	0
Base layer	ϵ_2	0.11e-4
	d_2	0.04e-4
Subgrade layer (soil)	ϵ_3	0
	d_3	—

Table 4.5: Percentage quadratic error for third approach

Figure 4.13: Better error function by generation for 5 variables using a frequency summation with $f_c = 1.5GHz$

4.3.3 Complete problem with white random noise

The third test is performed on the same way of the second one but, this time, a white noise of 1% is added to the original reflected electric signal of reference. DE parameters were maintained equals to the previous test. As a result of the DE algorithm execution, the figure 4.14 is obtained. In this figure the error function behavior referring to the generation is presented. As depicted, the number of maximum generation was reached and the algorithm stopped without the error condition being achieved.

Table 4.6 summarizes the obtained pavement parameters by the algorithm and the percentage quadratic error for each one. Given these results, it is possible to conclude that adding noise also results in a more complexity in the estimation process performed by the algorithm increasing the computational cost. However, the obtained values are really close to the reference ones which means that results are considered

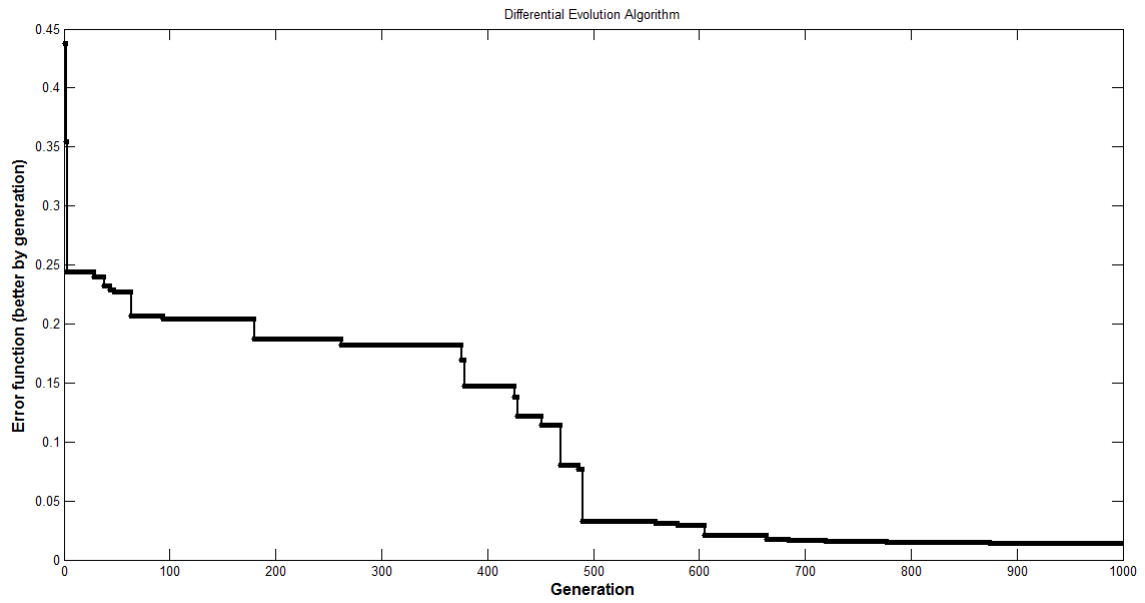


Figure 4.14: Better error function by generation for 5 variables using a frequency summation and a signal random noise.

satisfactory for this test.

	Variable	Obtained value	Error (%)
Asphalt layer	ϵ_1	6.01	0.002
	d_1	0.0799 m	5.05e-6
Base layer	ϵ_2	5.476	0.011
	d_2	0.252 m	0.195
Subgrade layer (soil)	ϵ_3	10.0920	0.084
	d_3	—	—

Table 4.6: Results of the complete problem with random noise

Chapter 5

Conclusions

This work proposed a comparative analysis of three different methodologies that intends to solve the multimodal inverse problem for GPR pavement parameter estimation. The main objective was to highlight in each studied approach, the advantages and disadvantages of their use. To achieve this, two techniques proposed in the literature were reproduced to solve the inverse problem. Also, a third one was derived from [Oliveira et al., 2014] by the author of this dissertation.

The first methodology consisted on a development in the time domain where some information about the reflected signal was taken to determine the pavement parameters. Through the amplitudes of the reflected pulses collected by an air-coupled GPR system and an equation proposed, the dielectric constants of all layers that composed a flexible pavement could be computed. In the same way, the pavement layers thickness could also be obtained by a single equation using the travel time from the wave. According to the results obtained by this technique, it was demonstrated that it is possible to find the quantities for the pavement structure employing this method. Nevertheless, two main drawbacks can make the method inaccurate. This is because all calculus made in this approach depend on the adequate detection of the reflected fields and the reflections can be affected by the width of the incident field and by noise. It was proved that if the working frequency is low and the pavement arrangement has a very thin layer, the reflected electric field signal will contain overlapped peaks that complicate the correct association of amplitudes values. In a similar way, noise is an intrinsic characteristic of measurements when these are carrying out. Thereby, the proper estimation will also represent a difficult task by employing this method.

The second method was a frequency domain approach that proposed to minimize the quadratic error function. It was established, for this frequency domain technique, that the error function presents characteristics of an ill-posed problem for layer thick-

ness variations. Then, it was suggested the use of a maximum GPR operation frequency ensuring this way the well-posedness of the problem. Besides, defining this maximum frequency leads to a unimodal characteristic of the function in the vicinity of the optimum point. This represents the major advantage of the technique, given that allows applying deterministic optimization tools, resulting in fast convergent methods. But also, it was proved that if the pavement variables range is small, it can be guaranteed a smooth function behavior giving the unimodal characteristic near to the optimum point region. However, the typical parameters found in the literature points to a wide range of them, which represents a significant drawback of this technique. Another disadvantage caused by the definition of the maximum frequency is the minimal size of the antenna, which will be limited. This makes the mobility difficult when measurements are being taken, and also, it limits the resolution of the environment being analyzed.

Finally, a third approach was presented in this work intending to take advantage of both methodologies in frequency and time domain. The inverse problem was also based on the error function analysis comparing the GPR data with the computational one, similarly to what was proposed in the frequency domain approach. However, employing the proposal allowed us to eliminate the limitation of the maximum frequency by using a frequency summation. This made it possible us to achieve the relaxation of the inverse problem which also leads to antennas size reduction given by the high frequency band reached with central frequency of 1.5 GHz. The main drawback of this technique was that the characteristic of unimodality was lost and it is not possible to use the deterministic algorithms to solve the problem anymore. Nevertheless, it didn't represent a big problem because a stochastic method (DE algorithm) could be used giving good results.

Consequently, this work allowed and evidenced that there are different methodologies that can be used in the attempt of solving the inverse problem generated by the wave propagation over multiple layers to elaborate non-destructive testing implying electromagnetic radiation. It was consigned here the main steps that can be used to reproduce any methodology and also its own advantages and disadvantages.

5.1 Further Work

The further work that can provide continuity to this thesis should develop more analysis in the matter.

- **Analysis of laboratory and real conditions problems.**

Measurements can be carried out in a laboratory or on the road directly, in order

to assess the performance of methods to real problems measured from the GPR.

- **Analysis of the viability of applying the propose to a large volume of data.** Tests on highways generates a very large data set and the optimization process can be computationally expensive. Since the highway do not normally have very large differences along itself, neighbor results may be used as starting points of the population and to analyze how it may accelerate the processing of the data, taking into account the convergence time of the method.
- **New techniques of frequency components combination.**
Use different ways to treat these components in order to analyze the variation in the objective function seeking to extend the space in the optimum point. Some techniques can be:
 - Use of prime frequency components.
 - Continuous spectrum.

Bibliography

- [Africano and Adriano, 2014] Africano, M. V. and Adriano, R. L. S. (2014). A Multimodal Inverse Problem for GPR Pavement Parameter Estimation. In *MOMAG 2014: 16° SBMO - Simpósio Brasileiro de Micro-ondas e Optoeletrônica e 11° CBMag - Congresso Brasileiro de Eletromagnetismo*, pages 606–609, Curitiba.
- [Agência Nacional de Transportes Terrestres, 2013] Agência Nacional de Transportes Terrestres (2013). Relatório anual.
- [AL-Qadi and Lahouar, 2005] AL-Qadi, I. and Lahouar, S. (2005). Measuring layer thicknesses with GPR - Theory to practice. *Construction and Building Materials*, 19(10):763–772.
- [Balanis, 1989] Balanis, C. A. (1989). *Advanced engineering electromagnetics*, volume 20. Wiley New York.
- [Bazaraa et al., 2006] Bazaraa, M. S., Sherali, H. D., and Shetty, C. M. (2006). *Non-linear Programming - Theory And Algorithms*. John Wiley & Sons, New Jersey, third edition.
- [Benedetti et al., 2006] Benedetti, M., Donelli, M., Martini, A., Pastorino, M., Rosani, A., and Massa, A. (2006). An innovative microwave-imaging technique for nondestructive evaluation: applications to civil structures monitoring and biological bodies inspection. *Instrumentation and Measurement, IEEE Transactions on*, 55(6):1878–1884.
- [Benedetto and Benedetto, 2002] Benedetto, A. and Benedetto, F. (2002). GPR experimental evaluation of subgrade soil characteristics for rehabilitation of roads. *Ninth International Conference on Ground Penetrating Radar*, 4758:708–714.
- [Biskup et al., 2005] Biskup, K., Lorenzo, H., and Arias, P. (2005). Aplicabilidad del radar de subsuelo para el estudio de la zona no saturada del suelo: ejemplos en

- ambientes arenosos costeros. *Estudios en la Zona No Saturada del Suelo*, VII:197–204.
- [Bohidar and Hermance, 2002] Bohidar, R. N. and Hermance, J. F. (2002). The GPR refraction method. *Geophysics*, 67(5):1474–1485.
- [Brough et al., 2003] Brough, M., Stirling, A., Ghataora, G., and Madelin, K. (2003). Evaluation of railway trackbed and formation: a case study. *NDT&E International*, 36:145–156.
- [Bush, 1989] Bush, A. J. (1989). *Nondestructive testing of pavements and backcalculation of moduli*, volume 1026. ASTM International.
- [Colagrande et al., 2011] Colagrande, S., Ranalli, D., and Tallini, M. (2011). Ground Penetrating Radar Assessment of Flexible Road Pavement Degradation. *International Journal of Geophysics*, 2011:1–11.
- [DasGupta, 2014] DasGupta, D. (2014). *Artificial immune systems and their applications*. Springer Publishing Company, Incorporated.
- [Fauchard et al., 2003] Fauchard, C., Dérobert, X., Cariou, J., and Cote, P. (2003). GPR performances for thickness calibration on road test sites. *NDT&E International*, 36:67–75.
- [Gentili and Spagnolini, 2000] Gentili, G. G. and Spagnolini, U. (2000). Electromagnetic Inversion in Monostatic Ground Penetrating Radar : TEM Horn Calibration and Application. *IEEE Transactions on Geoscience and Remote Sensing*, 38(4):1936–1946.
- [Gomez López, 2008] Gomez López, R. (2008). *Aplicación del radar de penetración en tierra (georadar) a la exploración no destructiva de yacimientos arqueológicos*. PhD thesis.
- [Hartman et al., 2004] Hartman, A., Baston-Pitt, J., Sedgwick, A., and Böhmer, G. (2004). PILOT STUDY ASSESSING THE FEASIBILITY OF ADVANCED GROUND PENETRATING RADAR IN PAVEMENT ASSESSMENT. In *Proceedings of the 8th Conference on Asphalt Pavements for Southern Africa (CAPSA '04)*, number September, pages 6–11, Sun City, South Africa.
- [Hidalgo et al., 2010] Hidalgo, C., Pandales, C. A., Pedroza, B. A., and Rodriguez, M. A. (2010). Comportamiento de una pista experimental de pavimento flexible con base estabilizada con cal. *Revista Ingenierias Universidad de Medellin*, 9(16):37–47.

- [Hoffmann et al., 1993] Hoffmann, L., Shukla, A., Peter, M., Barbiellini, B., and Manuel, A. A. (1993). Linear and non-linear approaches to solve the inverse problems: applications to positron annihilation experiments. *Nuclear Instruments & Methods in Physics Research*, 335:276–287.
- [Huang, 2004] Huang, Y. H. (2004). *Pavement Analysis and Design*. Pearson Prentice Hall, United States of America, second edition.
- [Hunaidi, 1998] Hunaidi, O. (1998). Evolution-based genetic algorithms for analysis of non-destructive surface wave tests on pavements. *NDT & E International*, 31(4):273–280.
- [Iswandy et al., 2009] Iswandy, A., Awangku, S., and Setan, H. (2009). GROUND PENETRATING RADAR (GPR) FOR SUBSURFACE MAPPING: PRELIMINARY RESULT. *Geoinformation Science Journal*, 9(2):45–62.
- [Keilis-Borok and Yanovskaya, 1995] Keilis-Borok, V. and Yanovskaya, T. (1995). Inverse problems of seismology (structural review). In *Computational seismology*, pages 109–113. Springer.
- [Khoury et al., 2014] Khoury, S., Aliabdo, A. A.-H., and Ghazy, A. (2014). Reliability of core test - Critical assessment and proposed new approach. *Alexandria Engineering Journal*, 53(1):169–184.
- [Kurtz et al., 2006] Kurtz, J. L., Fisher III, J. W., Skau, G., Armaghani, J., and Moxley, J. G. (2006). Advances in ground penetrating radar for road subsurface measurements. *SPIE*, 3066:11–21.
- [Lahouar and Al-Qadi, 2008] Lahouar, S. and Al-Qadi, I. L. (2008). Automatic detection of multiple pavement layers from GPR data. *NDT & E International*, 41(2):69–81.
- [Loizos and Plati, 2007] Loizos, A. and Plati, C. (2007). Accuracy of pavement thicknesses estimation using different ground penetrating radar analysis approaches. *NDT & E International*, 40(2):147–157.
- [Loulizi et al., 2003] Loulizi, A., Al-qadi, I. L., and Lahouar, S. (2003). Optimization of Ground Penetrating Radar Data to Predict Layer Thicknesses in Flexible Pavements. *Journal of transportation engineering*, 129:93–99.

- [Maharaj and Leyland, 2010] Maharaj, A. and Leyland, R. (2010). The dielectric constant as a means of assessing the properties of road construction materials. In *Proceedings of the 29th Southern African Transport Conference (SATC)*, volume 0001, pages 487–498, Pretoria.
- [Markel et al., 2003] Markel, V. A., O’Sullivan, J. A., and Schotland, J. C. (2003). Inverse problem in optical diffusion tomography. IV. Nonlinear inversion formulas. *Optical Society of America*, 20(5):903–912.
- [Menke, 1989] Menke, W. (1989). *Geophysical Data Analysis: Discrete Inverse Theory*. Academic press, San Diego, revised edition.
- [Michalewicz, 1996] Michalewicz, Z. (1996). *Genetic algorithms+ data structures= evolution programs*. Springer Science & Business Media.
- [Molyneaux et al., 1995] Molyneaux, T. C. K., Millard, S. G., Bungey, J. H., and Zhou, J. Q. (1995). Radar assessment of structural concrete using neural networks. *NDT&E International*, 28(5):281–288.
- [Morey, 1998] Morey, R. M. (1998). Ground Penetrating Radar for evaluating subsurface conditions for transportation facilities. Technical report, National Cooperative Highway Research Program, Washington, DC.
- [Oliveira et al., 2014] Oliveira, D. B., a.G. Vieira, D., Lisboa, A. C., and Goulart, F. (2014). A well posed inverse problem for automatic pavement parameter estimation based on GPR data. *NDT & E International*, 65:22–27.
- [Onwubolu and Babu, 2013] Onwubolu, G. C. and Babu, B. (2013). *New optimization techniques in engineering*, volume 141. Springer.
- [Pascual-Marqui, 1999] Pascual-Marqui, R. D. (1999). Review of Methods for Solving the EEG Inverse Problem. *International Journal of Bioelectromagnetism*, 1(1):75–86.
- [Pastorino, 1998] Pastorino, M. (1998). Short-range microwave inverse scattering techniques for image reconstruction and applications. *Instrumentation and Measurement, IEEE Transactions on*, 47(6):1419–1427.
- [Pastorino et al., 2002] Pastorino, M., Caorsi, S., and Massa, A. (2002). A global optimization technique for microwave nondestructive evaluation. *Instrumentation and Measurement, IEEE Transactions on*, 51(4):666–673.

- [Price and Storn, 1997] Price, K. and Storn, R. (1997). Differential Evolution - A Simple and Efficient Heuristic for Global Optimization over Continuous Spaces. *Journal of Global Optimization*, (11):341–359.
- [Price et al., 2006] Price, K., Storn, R. M., and Lampinen, J. A. (2006). *Differential evolution: a practical approach to global optimization*. Springer Science & Business Media.
- [Qing, 2003] Qing, A. (2003). Electromagnetic Inverse Scattering of Multiple Two - Dimensional Perfectly Conducting Objects by the Differential Evolution Strategy. *IEEE Transactions on Antennas and Propagation*, 51(6):1251–1262.
- [Qing, 2006] Qing, A. (2006). Dynamic Differential Evolution Strategy and Applications in Electromagnetic Inverse Scattering Problems. *IEEE Transactions on Geoscience and Remote Sensing*, 44(1):116–125.
- [Queiroz et al., 2013] Queiroz, F., Vieira, D., and Travassos, X. (2013). Analyzing the relevant features of gpr scattered waves in time-and frequency-domain. *Research in Nondestructive Evaluation*, 24(2):105–123.
- [Queiroz et al., 2012] Queiroz, F., Vieira, D., Travassos, X., and Pantoja, M. (2012). A review of soft techniques for electromagnetic assessment of concrete condition. *Mathematical Problems in Engineering*, 2012.
- [Rao and Savsani, 2012] Rao, R. V. and Savsani, V. J. (2012). *Mechanical design optimization using advanced optimization techniques*. Springer Science & Business Media.
- [Rao and Rao, 2009] Rao, S. S. and Rao, S. (2009). *Engineering optimization: theory and practice*. John Wiley & Sons.
- [Rocca et al., 2011] Rocca, P., Oliveri, G., and Massa, A. (2011). Differential Evolution as Applied to Electromagnetics. *IEEE Antennas and Propagation Magazine*, 53(1):38–49.
- [Rodriguez et al., 2015] Rodriguez, J., Pantoja, M., Travassos, X., Vieira, D., and Saldanha, R. (2015). A prediction algorithm for data analysis in GPR-based surveys. *Neurocomputing*, 168:464–474.
- [Saarenketo and Scullion, 2000] Saarenketo, T. and Scullion, T. (2000). Road evaluation with ground penetrating radar. *Journal of Applied Geophysics*, 43(2-4):119–138.

- [Spagnolini, 1997] Spagnolini, U. (1997). Permittivity Measurements of Multilayered Media With Monostatic Pulse Radar. *IEEE Transactions on Geoscience and Remote Sensing*, 35(2):454–463.
- [Storn and Price, 1995] Storn, R. and Price, K. (1995). Differential Evolution-A simple and efficient adaptive scheme for global optimization over continuous spaces. Technical report, University of California, Berkeley.
- [Sutinen, 1992] Sutinen, R. (1992). *Glacial deposits , their electrical properties and surveying by image interpretation and Ground Penetrating Radar*. PhD thesis, University of Oulu.
- [Tarantola, 2005] Tarantola, A. (2005). *Inverse Problem Theory and Methods for Model Parameter Estimation*. SIAM, United States of America.
- [Travassos et al., 2009] Travassos, L., Vieira, D., Ida, N., and Nicolas, A. (2009). In the use of parametric and non parametric algorithms for the non destructive evaluation of concrete structures. *Research in Nondestructive Evaluation*, 20(2):71–93.
- [Vesterstrøm and Thomsen, 2004] Vesterstrøm, J. and Thomsen, R. (2004). A comparative study of differential evolution, particle swarm optimization, and evolutionary algorithms on numerical benchmark problems. In *Evolutionary Computation, 2004. CEC2004. Congress on*, volume 2, pages 1980–1987. IEEE.
- [Yaseen and AL-Slamy, 2008] Yaseen, S. G. and AL-Slamy, N. (2008). Ant Colony Optimization. *International Journal of Computer Science and Network Security*, 8(6):351–357.
- [Zumrawi, 2014] Zumrawi, M. M. E. (2014). Prediction of In-situ CBR of Subgrade Cohesive Soils from Dynamic Cone Penetrometer and Soil Properties. *International Journal of Engineering and Technology (IACSIT)*, 6(5):439–442.